Modeling Daily Plume Specific Smoke Concentrations for Health Effects Studies with Estimates of Fire Size, Plume Age, and Fuel Type

Sam D. Faulstich (1*), Matthew J. Strickland (2), Yan Liu (2), S. Marcela Loría-Salazar (3), Xia Sun (4,5), Ash B. Cale (6), Heather A. Holmes (1)

1: Department of Chemical Engineering, University of Utah, Salt Lake City, UT, USA

2: School of Public Health, University of Nevada-Reno, Reno, NV, USA

3: School of Meteorology, University of Oklahoma, Norman, OK, USA

4: Cooperative Institute for Research in Environmental Sciences, University of Colorado Boulder, CO, USA

5: NOAA/Global Systems Laboratory, Boulder, CO, USA

6: Department of Natural Resources and Environmental Science, University of Nevada-Reno, Reno, NV, USA

*Corresponding Author: sam.faulstich@utah.edu

Abstract

Inhaling smoke $PM_{2.5}$ can cause adverse health effects ranging from acute (e.g., lung irritation) to chronic (e.g., lung cancer). Acute health effects have immediate implications for public health, requiring rapid response to minimize harm during an exposure window. Estimating acute health effects requires short-term (e.g., daily) estimates of fire-specific smoke $PM_{2.5}$ concentrations at ground level. Any temporal discrepancy (e.g., missing fire emissions information) may result in underestimated smoke exposure in an epidemiology study. This paper introduces a method to estimate daily fire-specific $PM_{2.5}$ smoke concentration at ground level in the western US from 2007-2019 to provide smoke characterizations (i.e., exposure estimates) for time-series studies investigating acute health effects. The smoke exposure model incorporates data on fire characteristics, such as fuel type, fire size, and fire distance, enabling a more detailed analysis of health impacts. This method utilizes updated fire emissions information as inputs to an atmospheric dispersion model, which determines the concentration and location of wildfire smoke after transport. These results are combined with a Bayesian time-series model to determine the smoke-specific portion of $PM_{2.5}$ measured from nine ground-based EPA monitors in the western US. The Bayesian model includes meteorology and season to estimate the background $PM_{2.5}$ concentrations. Using this data set with retained fire characteristics provides valuable insight into the differences between $PM_{2.5}$ concentrations at different locations. We found that fires with the largest burned area during the study period (1,753-1,850 km^2) affected six of our nine stations, showing how widespread smoke impacts from large fires can be. The Lindon, UT station was impacted by the greatest number of fires over the period (398), but the average smoke $PM_{2.5}$ concentration per fire was ~2 $\mu g\ m^{-3}$ and the highest smoke $PM_{2.5}$ concentration was 35 $\mu g\ m^{-3}$. In comparison, the Carson City, NV station was impacted by less than half the number of fires over the study period (177), but the average smoke $PM_{2.5}$ concentration per fire was three times higher (~6 $\mu g\ m^{-3}$), and the highest smoke $PM_{2.5}$ concentration was 159 $\mu g\ m^{-3}$. These examples highlight two significantly different smoke exposure conditions that could plausibly lead to different health outcomes. Being able to investigate the health effects of the fire-specific smoke characteristics improves our understanding of the impacts of smoke exposure and ensures that management strategies are mitigating all possible outcomes of wildfires, including transported smoke.

Keywords: air quality exposure modeling, smoke plume transport, wildland fire, biomass burning, smoke $PM_{2.5}$, Bayesian time-series model.

Synopsis: Existing methods have limitations for estimating daily smoke exposure, due to remote sensing limitations, model uncertainties, and isolating smoke in ground-based measurements. We combine fire emissions, atmospheric modeling, and Bayesian statistics to estimate daily $PM_{2.5}$ smoke exposure.

1 Introduction

Inhalation of $PM_{2.5}$ from wildfire smoke poses significant health risks to humans [1–9], with impacts extending beyond the immediate fire location due to atmospheric transport [10–14]. The projected increase in wildfire frequency and intensity due to climate change [8,15–18] requires understanding both short-term (acute) and long-term (chronic) health effects. Acute effects, such as respiratory or skin irritation [19–21], demand immediate public health responses [22–24], unlike long-term health effects (i.e., chronic respiratory diseases) [25,26]. Research often prioritizes studying long-term health effects (i.e., monthly or annual exposure estimates) due to the challenges of obtaining the high-resolution temporal (e.g., daily) data needed to model smoke exposure for acute health effects studies [3,27–29].

Estimating acute smoke exposure is complex due to the uncertainties in estimating fire emissions [14,30–33] and the need for high-resolution spatial and temporal data, which often do not coexist [29,34–36]. Obtaining ground-level pollutant concentrations poses further challenges, as existing monitoring methods do not provide smoke-specific concentrations [37,38]. Current approaches combine remote sensing [14,39–42], air quality monitoring [43–45], and atmospheric modeling [14,46–49], but these approaches struggle to capture fine-scale exposure dynamics [31,50,51], particularly in remote areas [52–55] or areas of complex terrain [56–58] and introduce additional uncertainties [33,41,59,60]. Due to these limitations, many satellite-based exposure models provide annual or monthly estimates [73,74], and modeling acute, daily exposure with these methods can be highly biased. Furthermore, atmospheric models (e.g., CTMs and coupled fire-atmosphere models) have uncertainties because of the complexity of modeling smoke microphysics and transport (e.g., fire and smoke behavior over complex terrain [51]). These issues contribute to limitations in using satellite products and atmospheric models to estimate spatiotemporal smoke exposures. Additionally, some health effects studies use distance from the fire as a metric for exposure [53], which can bias health effects results.

To address challenges with remote sensing of fires and smoke-specific exposure estimates, we developed a comprehensive framework for estimating acute smoke exposure at EPA monitoring locations. By integrating fire emissions inventories, atmospheric modeling, and Bayesian statistical methods, the framework aims to isolate smoke $PM_{2.5}$ concentrations from other sources of $PM_{2.5}$ in ground-based air quality monitoring data. This approach improves existing methods that only use a single data source by combining high spatial and temporal resolution fire emissions products and accounting for cloud cover in missed fire detections from satellites in an atmospheric dispersion model to provide estimates of $PM_{2.5}$ linked to smoke plumes from specific fires. These smoke $PM_{2.5}$ estimates are calibrated to ground-level $PM_{2.5}$ concentrations at EPA monitors using a Bayesian statistical model that includes meteorological covariates to determine the expected $PM_{2.5}$ concentrations from all other sources. Because each fire is modeled individually, the PM2.5 concentrations are plume-specific. Using fire-specific smoke concentrations that are calibrated to ground-based monitors further improves estimates of smoke-specific $PM_{2.5}$ concentrations for health effects studies. These improvements allow for a more detailed investigation of acute smoke-related health impacts, which leads to a more complete understanding of the health impacts of smoke exposure.

2 Methods

We developed a novel method to estimate daily smoke plume-specific $PM_{2.5}$ concentrations at ground level. This approach leverages a data fusion method that combines data from ground-based EPA monitors and results from an atmospheric dispersion model. We use EPA monitoring sites as the locations to estimate smoke exposure because our method was developed to support time-series environmental epidemiology studies that investigate acute health endpoints. While this exposure is not representative of a personal exposure or a population-based exposure, we leverage the best available ground-based measurements to calibrate our dispersion modeling results. Therefore, our modeling approach provides plume-specific smoke exposures at EPA monitoring locations for time series epidemiologic studies. To model all smoke plumes from fires that impact the monitors in the study, a study domain that includes all upwind fires is needed. The spatial domain for the dispersion model and monitoring locations are shown in Figure 1. Our approach retains vital fire information related to location, size, and fuel type for each smoke plume, allowing further stratification of the smoke exposures for health studies.

2.1 Modeling Downwind Smoke Plume Transport Using an Atmospheric Dispersion Model

The Hybrid Single Particle Lagrangian Transport (HYSPLIT) [80] model simulates the transport of wildfire smoke $PM_{2.5}$ through the atmosphere. We applied HYSPLIT forward trajectories for each individual fire in the modeling domain (Figure 1), using the $PM_{2.5}$ emissions released from each fire as an input to simulate the smoke transport to downwind locations. We chose HYSPLIT as the atmospheric dispersion model due to its low computational requirement, which is essential for the volume of runs we performed (approximately 3,200 simulation days per year, from 2007 to 2019). Additionally, HYSPLIT has been used in previous air quality and smoke studies [81–85].

Information about the fire properties (i.e., fire location, estimated emissions) is required for HYSPLIT modeling. This information comes from a fire emissions inventory (FEI). To address some common issues with FEIs, a combined FEI was used that provides high spatial resolution (30m) and high temporal resolution (daily) data as an input for the atmospheric model; the FEI combination method is described in Faulstich et al., (2025) [86]. This FEI uses emissions estimates from the Wildland Fire Emissions Information System (WFEIS, [87]) which accounts for fuel loading, combustion type, and burned area. The FEI provides information on a single fire, allowing the smoke plume for each fire to be tracked individually, including when several smoke plumes mix in a downwind location. The individual fire level FEI information also allows for health models to be designed that can investigate the impacts of different fire and smoke types (described below in Section 2.4). The FEI information used as inputs to HYSPLIT are the $PM_{2.5}$ emissions rate per hour, daily burned area, fire heat emissions, and daily fire location.

Daily burned area from the FEI is used by HYSPLIT to distribute particles uniformly throughout the geographical location defined by the burned area. Fire location dictates the location of the particle release, which informs terrain and meteorological conditions. The North American Model (NAM) 12 km reanalysis data [88] provides the gridded meteorological conditions for the HYSPLIT simulations. These meteorological conditions provide information on atmospheric stability, which impacts the modeled plume rise in HYSPLIT. The plume rise calculations in HYSPLIT use the Briggs plume rise model, using heat release from the FEI to characterize the fire intensity and thus smoke plume buoyancy [89]. The PM2.5 emissions rate per hour defines the quantity of PM2.5 released.

A single HYSPLIT forward trajectory run was used for the duration of each fire as determined by the FEI. HYSPLIT runs used a full 3D particle model. NAM has a 3-hourly time resolution, so HYSPLIT trajectories are calculated at the same time interval. The hourly $PM_{2.5}$ emissions and heat release from the FEI were averaged to a three-hour time resolution to match the NAM data.

Post-processing steps are required for the HYSPLIT outputs. First, the HYSPLIT concentration data are assigned a geolocation using the static NAM grid. The regridding of the HYSPLIT output was based on which NAM grid centroid was nearest to the Lagrangian HYSPLIT data point. This creates a static model grid for the simulation period versus the dynamic Lagrangian grid used in HYSPLIT, where the grid changes as it is adapted to follow the particles in the flow. Second, the HYSPLIT output is paired with an EPA ground-based air quality monitor (whose locations are also paired to the NAM grid) to calibrate the outputs (described below in Section 2.3). Finally, the HYSPLIT concentrations are averaged by day and location, so there is only one concentration data point for each fire (per day and location).

2.2 Estimating Background $PM_{2.5}$ Concentrations at Ground-Based Monitors Using a Bayesian Time Series Model

A background model is used to determine the expected $PM_{2.5}$ concentration from other air pollution sources so that the impact of smoke can be isolated at each EPA monitor location. To isolate the smoke and non-smoke impacts and build the background $PM_{2.5}$ model, it is required to know which days do not have smoke impacting the ambient $PM_{2.5}$ concentrations. Two different data sources were used to determine days with $PM_{2.5}$ concentration from upwind fire emissions (smoke days) and remove them from the training dataset used to build the background $PM_{2.5}$ model. The first method uses a smoke filter with NASA AErosol RObotic NETwork (AERONET) ground-based sun photometer data, where the Ångström Extinction Exponent (AEE) is used as a qualitative smoke filter [71]. When AEE is larger than 1.7 (i.e., fresh smoke), the day is flagged as a smoke present; when it is less than 1.7, it is flagged as a non-smoke day. This smoke filter can be used when the smoke investigated is near the source of the fire (plume age on the order of one day or less) because the aging mechanism impacts AEE values as they increase in particle size. Note that smoldering smoke (wet fuels) can have AEE values as low as 1.5 [90]. However, we are not taking these cases into account for this study as the fuel sources for the western U.S. tend to be dry. For our study, the AERONET data is only available from the Reno, NV station (located 1.5 miles from the Reno, NV EPA station) from 2012 to 2019. The second method for determining smoke days, required when AERONET data was unavailable (i.e., all other locations besides Reno, NV), is to use the results of the HYSPLIT simulations described above. For this method, any day with $PM_{2.5}$ concentrations estimated by HYSPLIT at the EPA monitor location was considered a smoke day and removed from the background PM training model for that location.

Using only data from the non-smoke days, a Bayesian Structural Time Series (BSTS) model is used (R BSTS package [91]) to train a model that can estimate the expected background $PM_{2.5}$ concentrations. The BSTS model is a time series regression model that can capture multiple additive trends in the data using Bayesian methods [91], where the non-smoke days are used as the observed equation to model how the background PM2.5 concentration changes with time based on seasonal and meteorological predictors. Daily, ground-level $PM_{2.5}$ concentration measurements from EPA monitors accessed from the EPA Air Quality System (AQS) are used in the BSTS model. Values less than 2 μgm^{-3} are removed and considered to be below the instrument detection limit. The natural log of the daily non-smoke $PM_{2.5}$ concentrations are used as input observations for a linear regression model with a lag 7 autoregressive correlation structure. Daily average windspeed and temperature are included as regressors to improve the prediction, using data from the MesoWest [92] sensor closest to the EPA station. Using binary indicator variables to represent each season (i.e., winter, summer, fall, and spring) in the BSTS model, seasons and their interactions with the average temperature and wind speed were added to the regression. Including these covariates improves estimates of background $PM_{2.5}$, especially in regions with significant meteorological impacts on ambient air pollution concentrations. The BSTS model runs with 5,000 iterations, and the expected background $PM_{2.5}$ concentrations for each non-smoke day are predicted. This Bayesian background model statistically estimates the average amount of daily non-smoke $PM_{2.5}$ expected at the EPA air quality monitor. The non-smoke background $PM_{2.5}$ can be used to estimate the smoke specific impacts on $PM_{2.5}$ concentrations at an EPA monitor.

2.3 Estimating Smoke Exposure through Calibrating Atmospheric Dispersion Modeling Results to Ground-Based Monitors Using the Bayesian Background Model

The atmospheric dispersion results from HYSPLIT provide information on smoke days and smoke locations. The Bayesian background model provides estimates of the non-smoke $PM_{2.5}$ concentrations. Utilizing these two sources of information, we calibrate the daily HYSPLIT smoke $PM_{2.5}$ concentrations for individual plumes with the EPA ground-based air quality measurements to obtain an estimate of the smoke-specific $PM_{2.5}$ concentrations

We determine daily, calibrated plume-specific smoke $PM_{2.5}$ concentration at ground level using HYSPLIT results and EPA data with the following equation:

$$PM_{calibrated} = \frac{PM_{fire_i}}{PM_{total}} * PM_{smoke} \quad (1)$$

Where $PM_{calibrated}$ is the calibrated wildfire plume-specific smoke $PM_{2.5}$ (i.e., smoke exposure), PM_{fire_i} is the smoke $PM_{2.5}$ from a specific fire on that day, as estimated by HYSPLIT, PM_{total} is the $PM_{2.5}$ from all fire smoke plumes on that day estimated by HYSPLIT (i.e., the sum of all PM_{fire_i} for that day), and PM_{smoke} is the smoke-specific $PM_{2.5}$ from $fire_i$ determined using the background $PM_{2.5}$ model. PM_{smoke} is calculated as:

$$PM_{smoke} = PM_{OBS} - PM_{background} \quad (2)$$

Where PM_{OBS} is the $PM_{2.5}$ measurement for that day from the observation data source (in this study, the EPA monitor) and $PM_{background}$ is the background $PM_{2.5}$ for that day estimated from the BSTS model. Equation 1 results in an estimated plume-specific $PM_{2.5}$ concentration at ground level and provides calibrated smoke estimates for each smoke plume that is impacting the monitoring site that can be used as a surrogate for smoke exposure in a time-series epidemiology study.

2.4 Estimating Smoke Exposure by Fire Size, Fuel Type, and Plume Age Characteristics

Because the smoke $PM_{2.5}$ at each monitoring site can be traced back to the fire of origin, additional information on fire size, fuel type, and plume age characteristics further stratifies potential health effects. The fire size and fuel type both impact the types of emissions released during fuel burning, leading to different chemical compositions for the emitted and transported smoke $PM_{2.5}$ [93,94]. We hypothesize that these differences will result in different concentration-response functions for the $PM_{2.5}$ smoke exposure [95,96]; therefore, estimating the exposures for the different fire and plume characteristics aids in investigating the different health associations.

Fire size is tracked in the FEI as burned area. Burned area is crucial information to input to HYSPLIT when modeling smoke transport. Prescribed burns and wildland fires often differ in size and combustion temperature [51,91] because prescribed burns are managed, which leads to different fire characteristics, leading to different health impacts [97–99]. Smoldering and flaming combustion occur at different temperatures and thus create different smoke plume compositions [87,99,100]. In addition to fire size, combustion type is also related to fuel types, with prescribed and agricultural burns being more prone to smoldering combustion due to the fuel types in these fires [87,101,102].

Land cover type is an important metric as it represents fuel type, and different fuel types have smoke plumes with different health effects [17,99]. Despite the inability to remotely sense understory vegetation, it has been empirically shown that landcover of the overstory correlates with surface fuel type [103,104]. Additionally, changes in landcover type can alter fuel type and subsequently effect combusted material [105]. In this study, fire location centroids from each fire are used to derive landcover type from the National Land-Cover Database (NLCD). The NLCD is typically updated every two to three years to account for land use or land cover changes. Here, we use the most recent previously available data release (e.g., a 2017 fire will use the 2016 NLCD) in order to best account for fuel type at time of the fire [106]. Sometimes the land-use type characterization method places a fire in a cell that is identified as water. This is likely due to the resolution of the NLCD. If a cell is classified as open water, that likely means that the fire started close to a body of water where the whole cell is classified as water, though it might not be. This happens most often in areas with semi-ephemeral streams or small riparian areas. These fires are retained in the FEI and the land-use type is not changed, so they are not included in the land-use type analysis.

Fresh versus aged plumes have different chemical compositions that can have different health impacts [95,107]. Here, we use a simple approach based on the distance from fire and average surface wind speed based on historical wind data from each state in the study domain [108] because the HYSPLIT trajectory calculation does not include the time of arrival of a specific particle at a specific location. The location of each fire on each day was used to determine the distance between the fire and the EPA station, and this distance was multiplied by the average daily wind speed to estimate how many days the smoke was transported for. This plume age estimation method does not account for wind direction. However, smoke from downwind fires are not in the final exposure dataset, because the HYPLIT trajectories account for the upwind/downwind differences in smoke transport. While this method is simplistic, it still provides initial estimates on plume age that may impact the health effects of inhaling fire smoke.

3 Results and Discussion

3.1 Modeling Downwind Smoke Plume Transport Using an Atmospheric Dispersion Model

An evaluation of the HYSPLIT modeling results compared to the EPA ground-based monitoring data allows for an understanding of how well the atmospheric dispersion model captures elevated $PM_{2.5}$ concentrations from smoke plumes. The HYSPLIT results and EPA ground-based monitoring data correlate ($R = 0.27$, $R^2 = 0.09$), shown in Figure 2 for all stations. This correlation indicates that the HYSPLIT atmospheric dispersion model represents temporal trends similar to the ground-based observations. This correlation can be calculated for each EPA monitor in the domain, and the range of correlations (R) is 0.034-0.52 (Figures S1-S9 in the Supporting Information). While the correlations are low, the smoke plumes from HYSPLIT generally agree with elevated smoke days in the EPA observations, and the relationship between the two variables is statistically significant ($p < 0.05$).

The HYSPLIT results are used to determine smoke $PM_{2.5}$, so determining how often the smoke days agree (i.e., binary smoke, non-smoke categorization) between HYSPLIT and the observations is another useful indicator of the model performance. We use the 2006 World Health Organization 24-hour ambient air quality guideline of 25 $\mu g\ m^{-3}$ [109] to classify smoke days in the EPA ground-based observations. The 2006 guidelines were chosen because it is the relevant recommendation for the study period, where any $PM_{2.5}$ measurement above 25 $\mu g\ m^{-3}$ is considered a smoke day for comparison with the HYSPLIT results. Although we quantify the agreement between this 25 $\mu g\ m^{-3}$ cutoff and our HYSPLIT estimates, we note that the EPA data is not smoke specific and thus not suitable to directly use as smoke exposure estimates – it simply indicates dates with elevated $PM_{2.5}$ concentrations. EPA and HYSPLIT smoke indicators agree on the smoke and non-smoke impacted days 74.4% of the time across all stations from 2012 to 2019 (Figure 3). Across all stations, the EPA data has more smoke days than HYSPLIT. This is because the EPA data is not smoke-specific, so some of the high $PM_{2.5}$ days flagged as smoke in the EPA data can be other high $PM_{2.5}$ days, such as wintertime inversions or dust. Approximately 73.5% of the days where the EPA monitor flags smoke when HYSPLIT does not occur in November, December, and January, pointing to high $PM_{2.5}$ caused by wintertime inversions. Additionally, the average estimated $PM_{2.5}$ smoke exposure on days when HYSPLIT detects smoke, but the EPA does not, is 0.68 $\mu g\ m^{-3}$. This low concentration indicates that the smoke exposure estimates resulting from smoke/non-smoke misclassifications in the background model do not represent significant exposure (i.e., concentrations less than the $PM_{2.5}$ instrument detection limit).

These findings indicate that HYSPLIT is an effective atmospheric dispersion model to use for estimating smoke exposures. The correlation between the HYSPLIT results and EPA data (Figure 2) illustrates that these two data sources capture similar trends in $PM_{2.5}$ at these locations. The comparison of smoke/non-smoke agreement/disagreement between the two data sources (Figure 3) shows that HYSPLIT often captures the same smoke days as the EPA monitors, with some discrepancy accounting for the fact that the EPA smoke days include high $PM_{2.5}$ days from other sources or events (e.g., winter inversions and dust). In the future, using a more advanced plume rise characterization within HYSPLIT can better represent the complexities of plume rise, which can vary based on fire characteristics and atmospheric conditions. While the Briggs plume rise model is standard in atmospheric modeling (i.e., regional and global CTMs), there has been recent research focused on improvements in other atmospheric models [77] and within HYSPLIT [110].

3.2 Estimating Background $PM_{2.5}$ Concentrations at Ground-Based Monitors Using a Bayesian Time Series Model

We also evaluate the Bayesian background model to further understand the uncertainties in the exposure modeling results. One way to assess the background model is to use data withholding. This technique allows some data (in this case, 20% of the data, selected randomly) to be set aside during model building so that the data can then be used for comparison purposes. Data withholding results for each station show that the average R^2 value for all stations is 0.69 (+/- 0.21). The average normalized mean bias for each station is -7.46 (+/- 2.74), and the average root mean squared error is 5.2 $\mu g\ m^{-3}$ (+/-1.84 $\mu g\ m^{-3}$), meaning that our model captures the variables that cause the variance in the background $PM_{2.5}$. Figures showing the bias, error, and correlation for each station are shown in the Supporting Information (Figures S10-S18).

External datasets of smoke days can provide additional insight into the performance of the Bayesian background model. Compared to an additional dataset of smoke day characterizations, HYSPLIT misses some smoke days in Reno. When comparing HYSPLIT smoke results to AERONET smoke detections in Reno, HYSPLIT and AERONET agreed on smoke days 71% of the time from 2012 to 2019. This is less agreement than is seen between the EPA dataset for Reno. Because the AERONET dataset is only available in Reno, this comparison is only possible for the Reno station, but it shows that our model captures smoke classifications in the Reno area similarly to an external dataset. HYSPLIT can miss smoke days due, in part, to uncertainties in the Eulerian meteorological model (i.e., the gridded NAM regional scale reanalysis model) used to drive the Lagrangian dispersion model. The missed smoke days also impact the background model, resulting in a higher estimated background PM than if all smoke days were excluded.

The Bayesian background model is helpful for creating exposure estimates that are smoke-specific. In the future, additional work on the Bayesian model can improve the background $PM_{2.5}$ estimates. For example, including more information on smoke days from other data sources when available, or filtering out high $PM_{2.5}$ days as smoke days in the EPA observations could improve the background estimates. Further investigation of disagreement days between HYSPLIT and EPA through FRP or $PM_{2.5}$ chemical speciation data can also provide additional value to the Bayesian model by further validating the smoke days dataset. Adding additional covariates that characterize the other non-smoke sources of air pollution emissions would also lead to better background $PM_{2.5}$ estimates. Additionally, while the EPA ground-based monitoring network is extensive, many rural locations lack EPA stations, meaning that this method cannot be applied in these areas to estimate smoke exposure without using a spatial dataset (e.g., atmospheric or land use regression model) to calibrate the background $PM_{2.5}$ concentrations. Using spatially resolved air pollution concentration data with the Bayesian model would also allow for the smoke exposures to be estimated at locations that do not have EPA monitors.

3.3 Estimating Smoke Exposure through Calibrating Atmospheric Dispersion Modeling Results to EPA Data Using the Bayesian Background Model

Figure 4 shows the distribution of high smoke exposure days, defined as smoke $PM_{2.5}$ greater than 25 $\mu g\ m^{-3}$, at each station. Each station has a different number of high exposure days, showing that exposure to wildfire smoke varies by location. Fresno, CA had the highest number of high exposure days over the study period with 39 days with exposure greater than 25 $\mu g \, m^{-3}$. Carson City, NV had the only smoke exposure day over 150 $\mu g \, m^{-3}$. This stratification shows the advantage of determining smoke exposure at individual locations, because while Carson City had the highest smoke exposure day, Fresno had more frequently occurring high smoke exposure days, which may point to more exposure overall and thus differing health effects.

Figure 5 shows the distribution of the number of fires with smoke impacting each station. The results show that each station is impacted by both a different number of fires and a different amount of smoke exposure from each fire. Sparks, NV; Fresno, CA; and Lindon, UT had the highest number of fires with smoke plumes impacting the monitor over the study period, with 263, 270, and 398 fires respectively. While they had the highest number of fires, these fires were primarily associated with smoke plumes that had less than 50 $\mu g \, m^{-3}$ of smoke exposure. This stratification exemplifies the variety of exposures and subsequent health effects to be accounted for. The health consequences of frequent exposure to a small amount of smoke may be different than the consequences of less frequent exposure to a high amount of smoke.

Figure 6 shows that each station is impacted by smoke from fires that are a range of distances away (100-1,000,000 m). This potentially causes differences in exposure due to the chemical evolution of the smoke plume as it is transported downwind. Additionally, smoke from a single fire may be detected at more than one station. As the smoke is transported through the atmosphere, the chemical aging of the plume may mean that smoke from one fire can cause different health impacts at different locations.

3.4 Estimating Smoke Exposure by Fire Size, Fuel Type, and Plume Age Characteristics

By including additional data sources in our exposure modeling framework, we can track the fuel type, fire size, and plume age for each smoke plume and exposure estimates, which can be used to investigate patterns in the dataset. Figure 7 shows the distribution of the burned area of the fire that resulted in smoke exposure at each station. The smoke exposures associated with the largest burned area (1,753-1,850 km^2) affected Carson City, Reno, Sparks, Modesto, Fresno, and Bakersfield, showing how widespread the smoke impacts from a single fire can be. The differences in fire sizes creates differences in the smoke plume composition due to differences in combustion characteristics associated with fire size [111–114]. Because of these differences in the composition of the smoke plume, it is possible that there are differences in health effects from smoke plumes resulting from different fire sizes. Since this dataset retains information on fire size from each fire, it is possible to estimate smoke exposure based on fire size.

The fire size information can be combined with fuel type information, also included in our exposure model, to estimate which fires could be prescribed or agricultural burns and which fires are wildfires. In the western US, fires that are smaller in size (less than 3.6e+05 m^2) [115] with shrub/scrub fuels are likely prescribed burns. Also, small fires with cultivated crop fuels are likely agricultural burns [112]. Understanding the health impacts of smoke from prescribed fires is important for land management and policy decisions. Our model provides the combined estimates of fire size and fuel type that can be used to identify smoke from prescribed fires. In our dataset, the most common fuel type for smoke exposures over the study period was evergreen forest (Figure 8). The EPA station most impacted by smoke from fires burning evergreen forest was Modesto, CA. This station also had many smoke impacts from cultivated crops, meaning that Modesto is likely impacted by both wildfire smoke and agricultural/prescribed burning.

The land use classification makes it possible to gain more insight into smoke exposure trends. Based on Figure 4, the station that had the highest smoke exposure days was Fresno, California. Fresno is also frequently impacted by smoke from cultivated crops, meaning they experience impacts from wildfire and agricultural burning. Fresno is located in Tulare County, which has a higher poverty rate than the other locations in our study [116]. Because the health impacts of wildfire smoke vary by socio-economic status (SES) [117], it is possible that Fresno may experience worse health impacts, both because of the frequency of smoke plumes in the area and the SES of the area. Future work in this area could include classifying landcover type for each daily fire location, which would allow deeper understanding of the fuel characteristics of each day of the fire and tracking of changes as the fire progresses.

Plume age is an additional piece of information included in this dataset. The chemical composition of the smoke plume changes as it ages and moves through the atmosphere [93,95,118]. Most smoke stays in the atmosphere for two days or less before being detected at ground level (Figure 9), but there are some fires that are estimated to be aged as much as five days. Las Vegas, NV, was most frequently impacted by plumes that had been aged for five or more days (17 plumes). Lindon, UT, was most frequently impacted by plumes that had been aged for less than one day (208 plumes). The differences in health effects between fresh and aged plumes found in the literature [93–95] suggest that investigating the health effects between these two locations could provide an insightful comparison. The literature also disagrees on whether aged smoke is better or worse than fresh smoke based on the compound of interest [117], so comparing these two locations can provide valuable insight into the health outcomes experienced by a population. Because our dataset tracks plume age, this comparison of plume age and health effects by location is made possible.

The novel method for estimating wildfire smoke exposure presented in this paper helps to address data gaps, such as missing fires, that affect acute smoke exposure studies. Our method also includes additional information on fires that allows for health studies to be designed to investigate the health associations of smoke exposures resulting from different fire characteristics. This method also calibrates the smoke exposure estimates using real-world $PM_{2.5}$ observations, which is highly advantageous when working with fire emissions and smoke transport, where the uncertainty of model estimates benefits greatly from the inclusion of real-world data.

4 Implications for Smoke Exposure Modeling

Previous smoke studies have variably relied on fire information that is incomplete due to remote sensing challenges [119], focused exclusively on long-term health effects [7,95,120], used short study time frames or small geographical areas [5,9,21,121,122], used a binary fire exposure term instead of a specific concentration estimate [53,123], or have not included exposure specific to each individual fire [40]. The new smoke exposure model in this paper advances the state-of-the art in smoke exposure modeling and provides advantages over simplistic methods used in some other health effects studies (i.e., using distance from fire as a metric for exposure). We include finer spatial resolution fire information and account for missing fire detections due to cloud cover, based on the FEI method in Faulstich et al., (2025) [86]. Therefore, less fire information is missing compared to using a single remote sensing method and without relying on visual fire identification methods (i.e., human detection). Using HYSPLIT to determine the atmospheric transport of wildfire smoke plumes means that the smoke estimates can be determined at ground level, where exposure occurs, versus a column-integrated value detected from satellite remote sensing. Additionally, by running HYSPLIT for each fire in the domain, we retain fire information (e.g., fuel type, fire size, and plume age) that allows for further stratification of the smoke exposure estimates. While CTMs can track the formation of secondary $PM_{2.5}$ from fire emissions and may run in higher resolution, it is not computationally feasible to track smoke from individual fires over a decade because it would require one CTM run for each fire in the domain. For example, in our simulations, we found that the average time for a single fire simulation day for our domain using HYSPLIT, running on a single CPU, was 3.6 minutes. For comparison, in a CTM model such as CMAQ, a single fire simulation day for the continental U.S. (CONUS, 12km horizontal resolution and 30 vertical levels) takes 4 hours on 64 CPUs. In this study, the average number of fire simulation days per year is approximately 3,300. For one year of simulation results, so HYSPLIT would take just over about 8 days of computational time (1 CPU), but CMAQ would take 1.5 years for the CONUS domain (64 CPUs).

The Bayesian background model also improves the background $PM_{2.5}$ estimates by including information on variables like season, temperature, and wind speed. These meteorological variables allow the Bayesian model to factor in conditions that may impact background $PM_{2.5}$ levels, as opposed to relying on historical averages of non-smoke estimates of $PM_{2.5}$ on the same day in other years [40,124,125]. Previous HYSPLIT studies often determined the origin of smoke using backward trajectories [81,126], but using back trajectories does not retain information on individual fire and smoke plume characteristics because it does not determine which specific fires resulted in the smoke exposure, especially in the case of overlapping plumes from multiple fires. Because fire size and combustion type can impact the composition of $PM_{2.5}$ and thus the health effects [97,127], the information on fire size, fuel type, and plume age enhances smoke exposure estimates by providing proxies of the different chemical compositions in smoke plumes.

Acknowledgements: Research reported in this publication was supported by the National Institute of Environmental Health Sciences (NIEHS) of the National Institutes of Health under award number R01ES029528. The support and resources from the Center for High Performance Computing at the University of Utah are gratefully acknowledged. We are grateful to the developers of WFEIS, who provide access to multiple data products to model fire emissions through one online platform. We are also grateful to the AERONET PIs and site managers.

This research utilized weather observations for stations in Nevada and California from RAWS and NWS networks and were obtained using the Synoptic Data PBC Mesonet API.

Data availability statement: The AERONET (https://aeronet.gsfc.nasa.gov) data used in this study are freely available from NASA. The fire emissions information data that supports this study can be found on the WFEIS website at https://wfeis.mtri.org/home. The EPA monitor data can be found on the EPA website at https://aqs.epa.gov/aqsweb/airdata/download_files.html.

Conflicts of Interest: The authors declare no conflicts of interest.

Figures

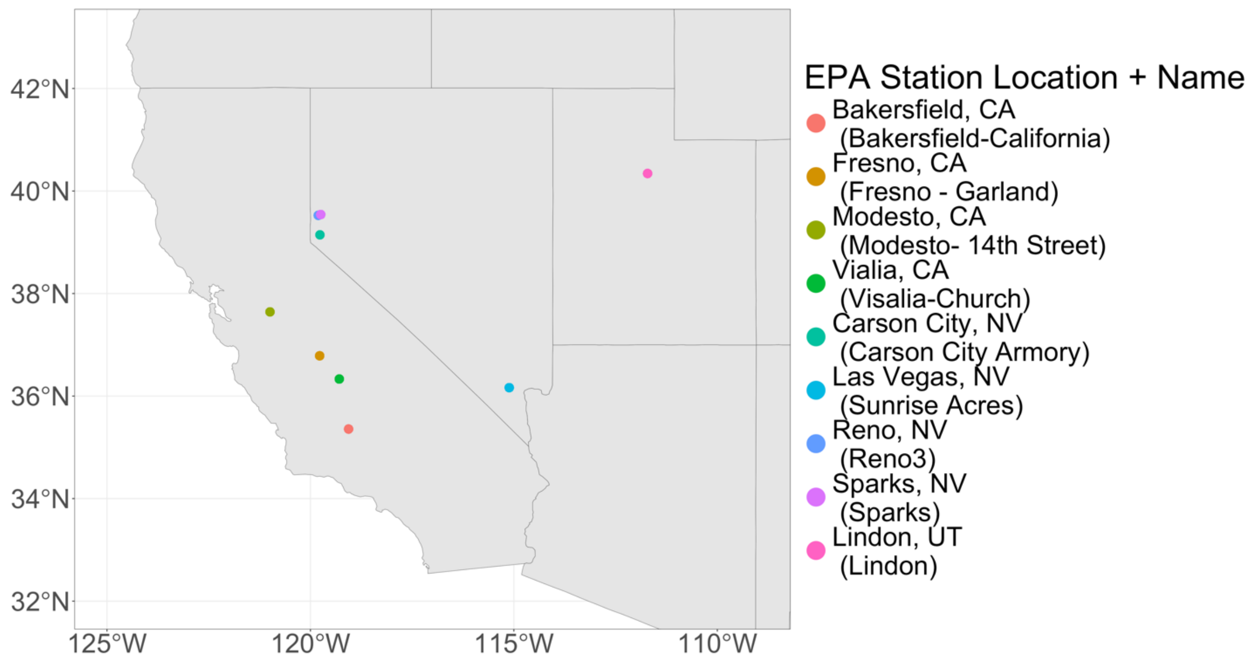

Figure 1. Map of EPA monitor locations used for analysis. This map also represents the spatial domain used for atmospheric modeling.

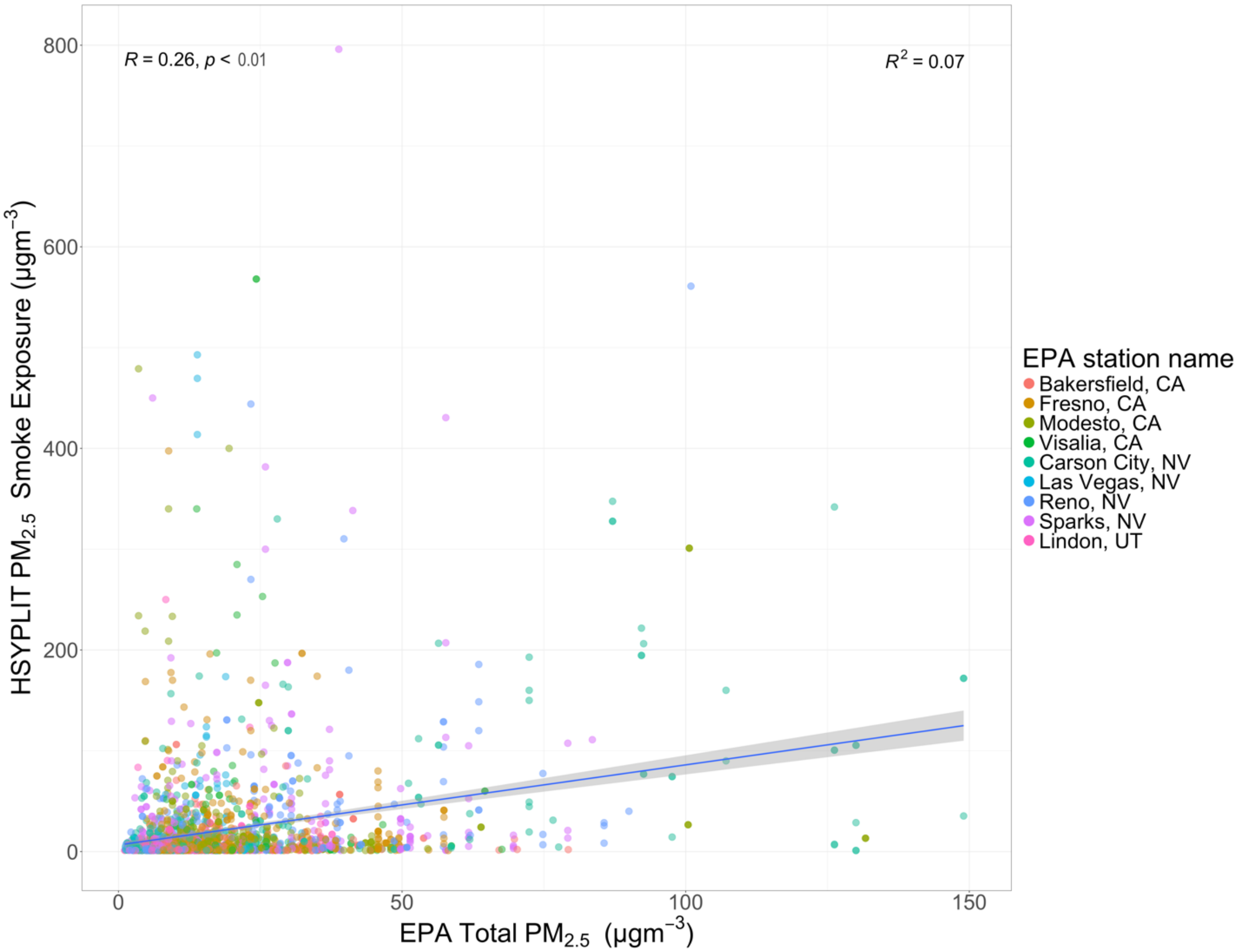

Figure 2. $PM_{2.5}$ concentrations ($\mu g\ m^{-3}$) from HYSPLIT compared to $PM_{2.5}$ concentrations ($\mu g\ m^{-3}$) from EPA station monitors. Note: The HYSPLIT results only account for $PM_{2.5}$ from smoke. The blue line shows a standard linear regression and the grey interval shows the 95% confidence interval of the model fit. The correlation coefficient (R) is 0.26, the statistical significance (p) is less than 0.01, and the coefficient of determination (R^2) 0.07.

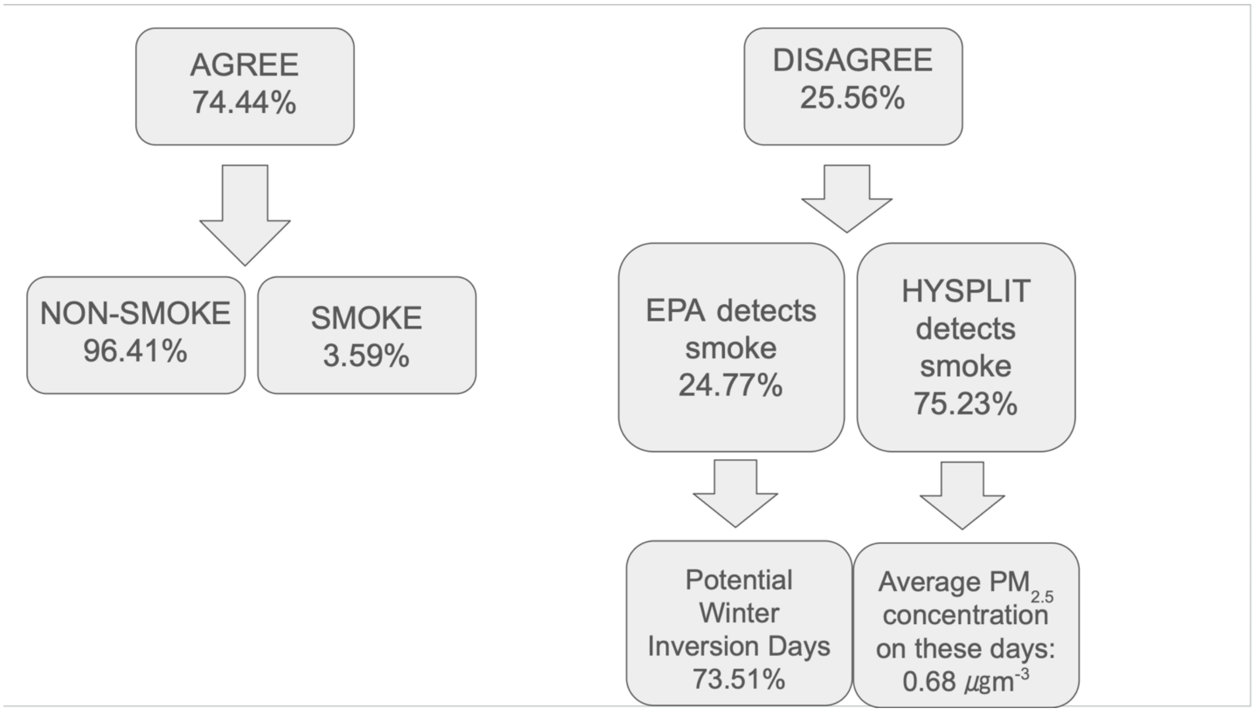

Figure 3. A schematic of daily "agree" and "disagree" indicators between HYSPLIT results and EPA monitor data to assess the model skill for smoke events. The average $PM_{2.5}$ concentration is the average of smoke exposure on all days that HYSPLIT detected smoke and the EPA did not. Note: The EPA data is not wildfire specific, meaning that it includes high $PM_{2.5}$ days from wintertime inversions and other pollution events.

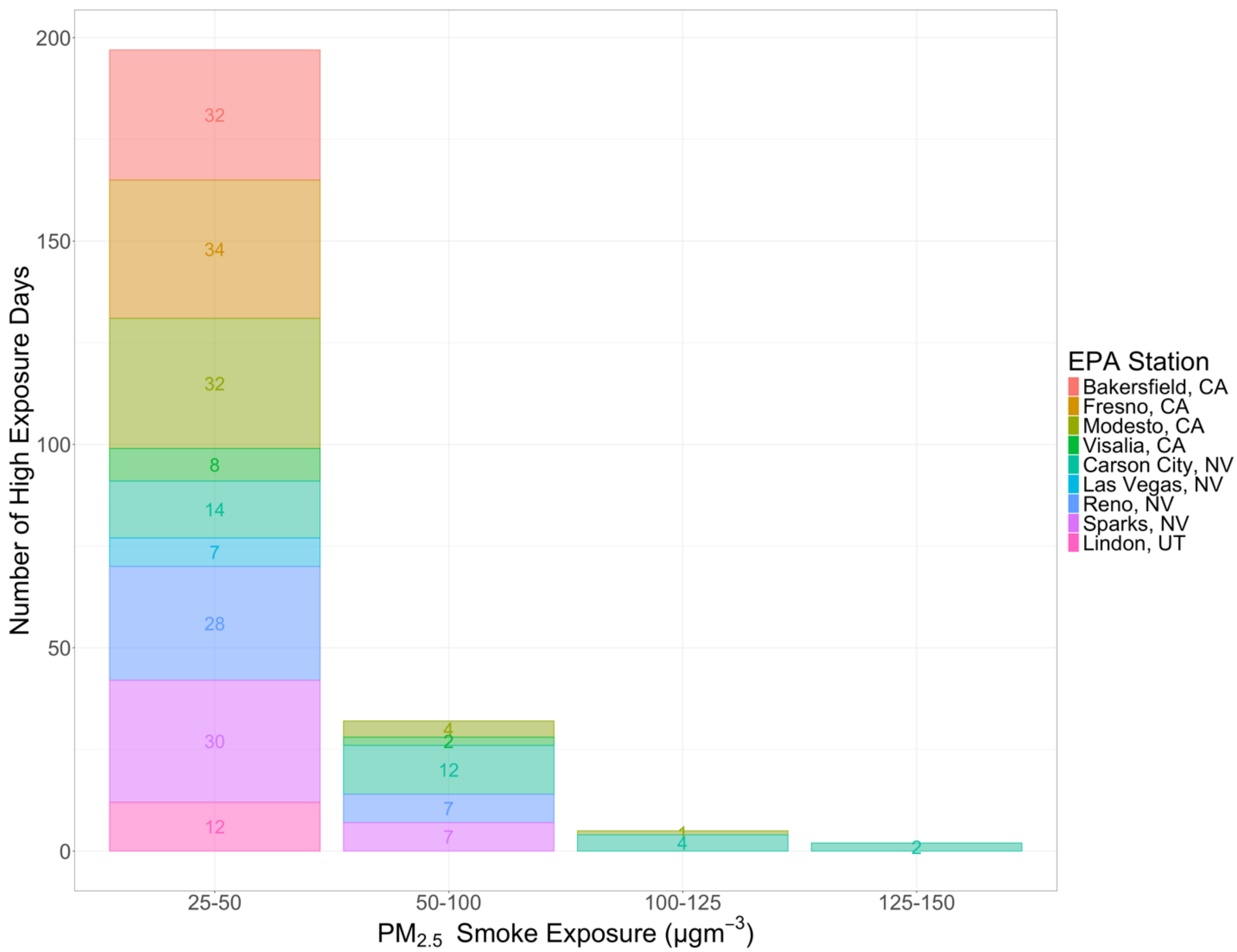

Figure 4. Distribution of smoke $PM_{2.5}$ exposure as estimated by HYSPLIT for high exposure days at each station during 2012 - 2019. High exposure is classified as $PM_{2.5}$ concentrations that exceed 25 $\mu g\ m^{-3}$, based on the World Health Organization 2006 guidelines [109].

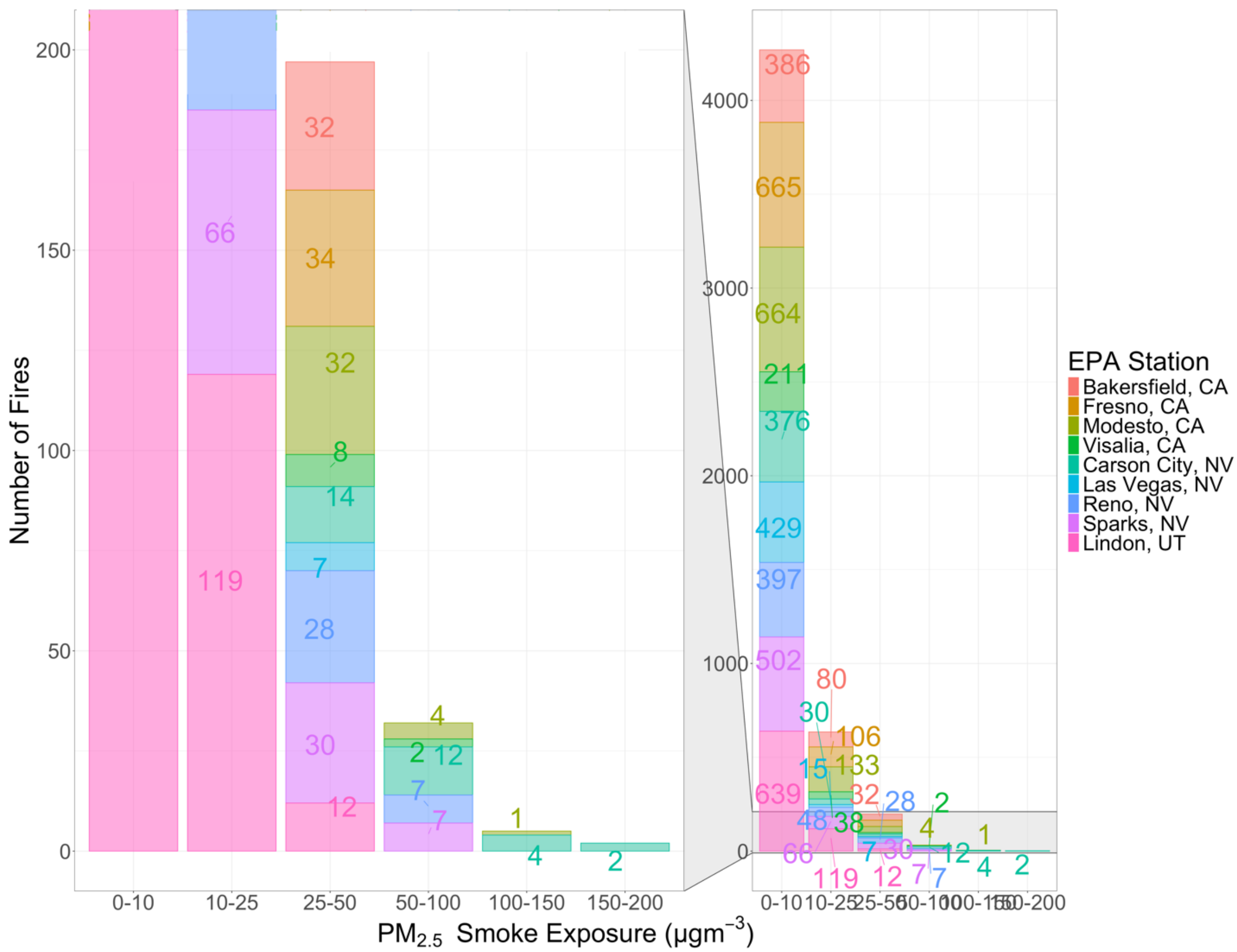

Figure 5. Distribution of the PM$_{2.5}$ smoke exposure as estimated by HYSPLIT impacting each station.

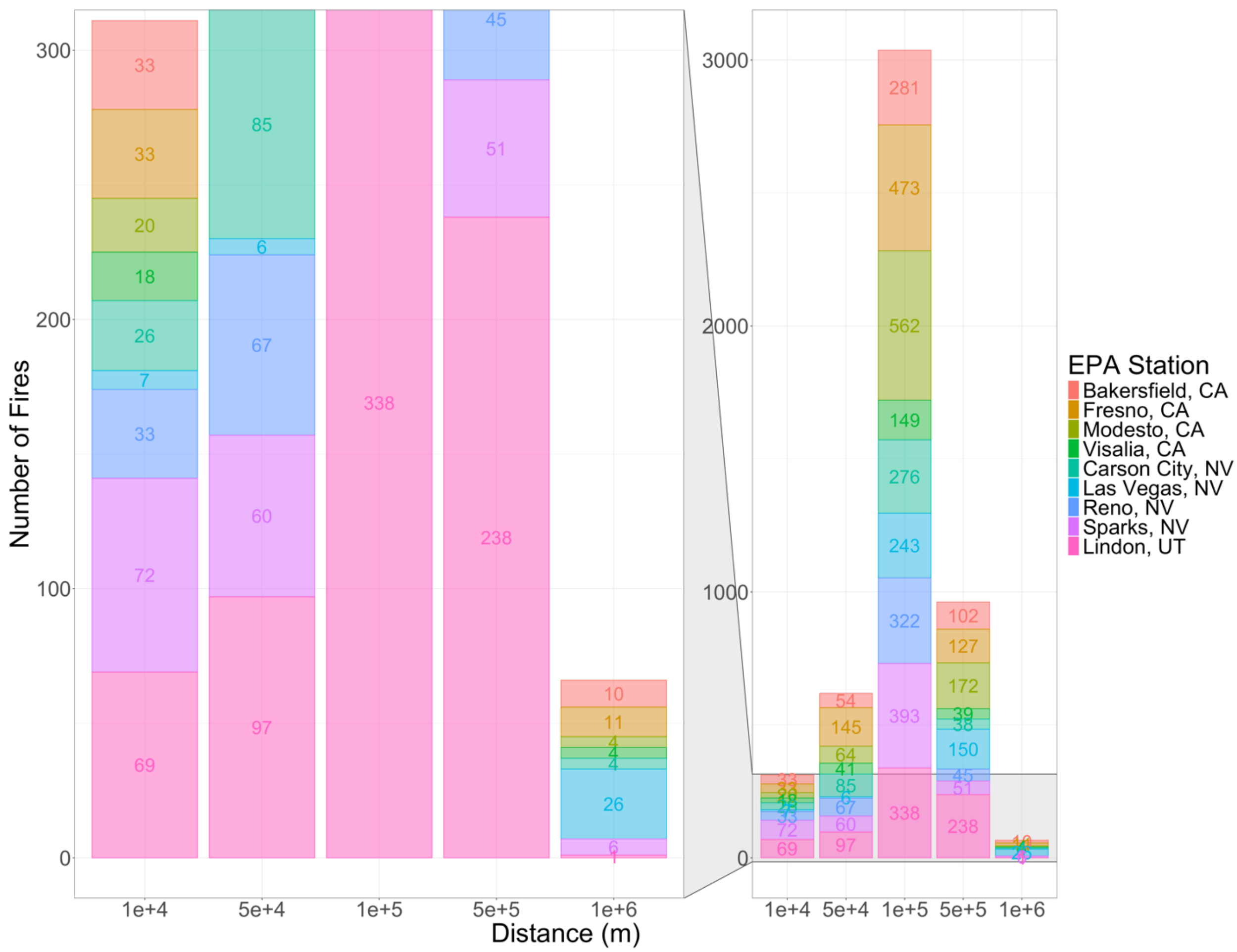

Figure 6. Distribution of the distance between the fire and EPA stations for fires contributing to smoke $PM_{2.5}$ exposure as estimated by HYSPLIT in each location.

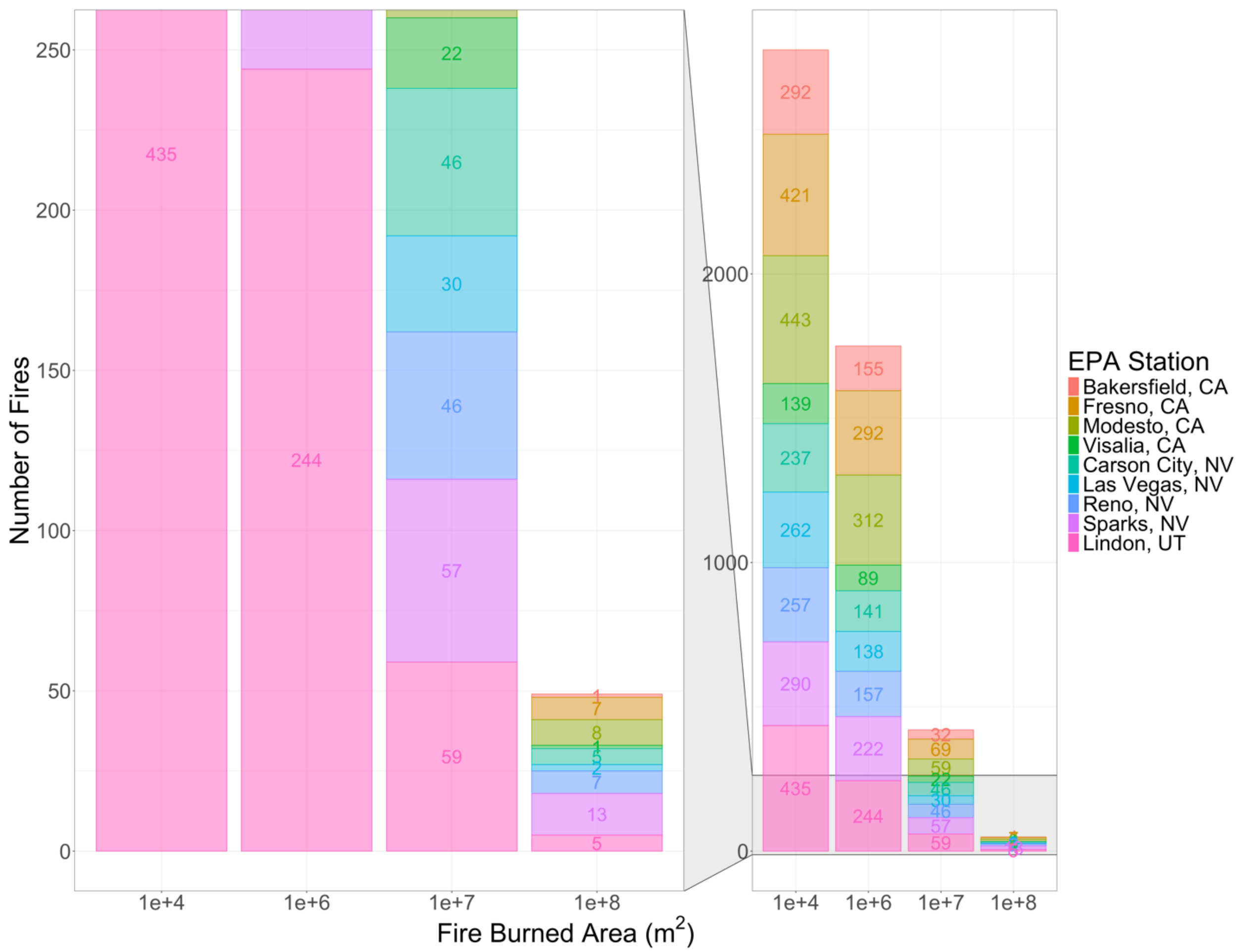

Figure 7. Distribution of the fire size, indicated by burned area, of the fires contributing to smoke $PM_{2.5}$ exposure as estimated by HYSPLIT in each location.

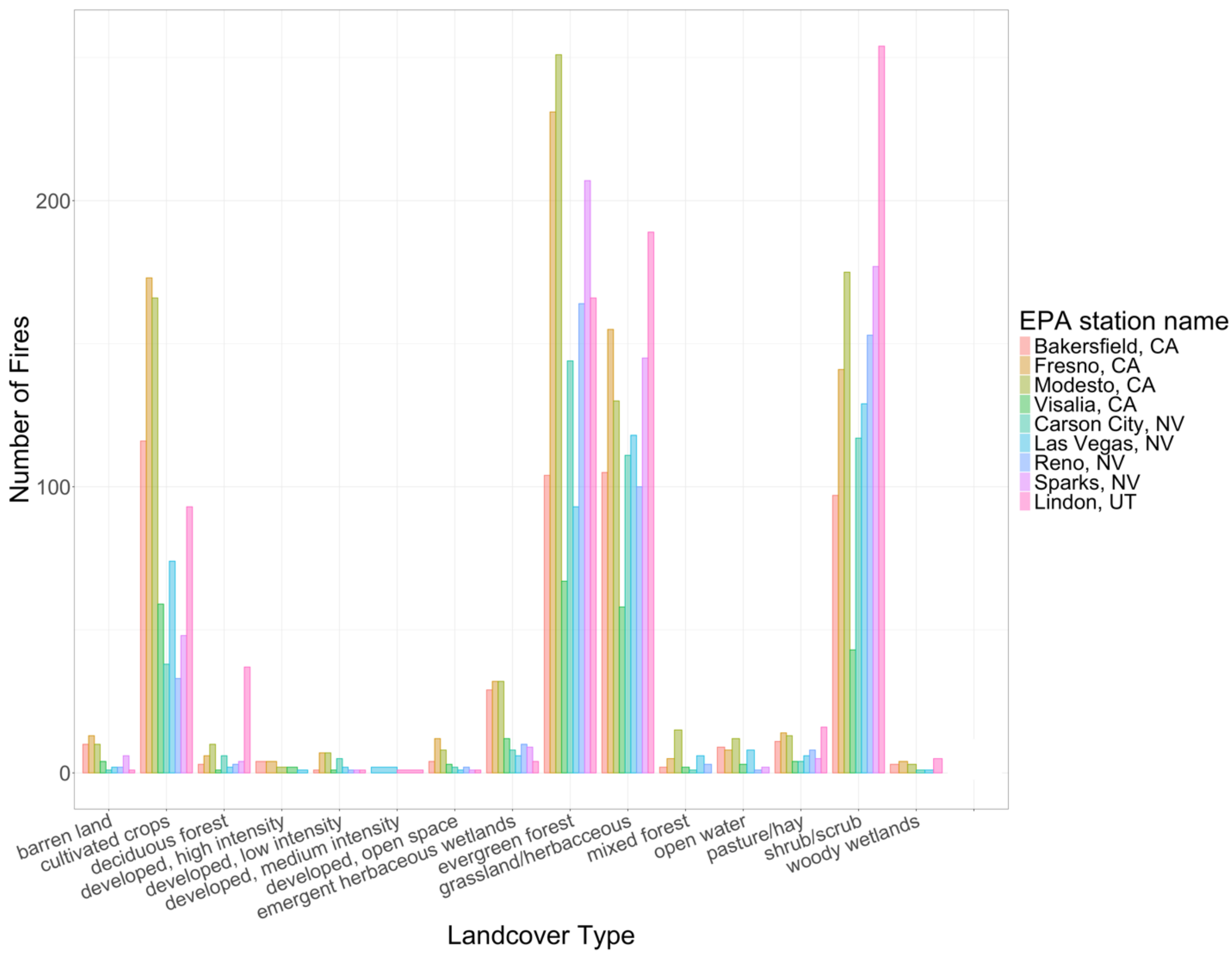

Figure 8. Distribution of the land cover type of each fire with smoke plumes that impacted each station from 2012-2019.

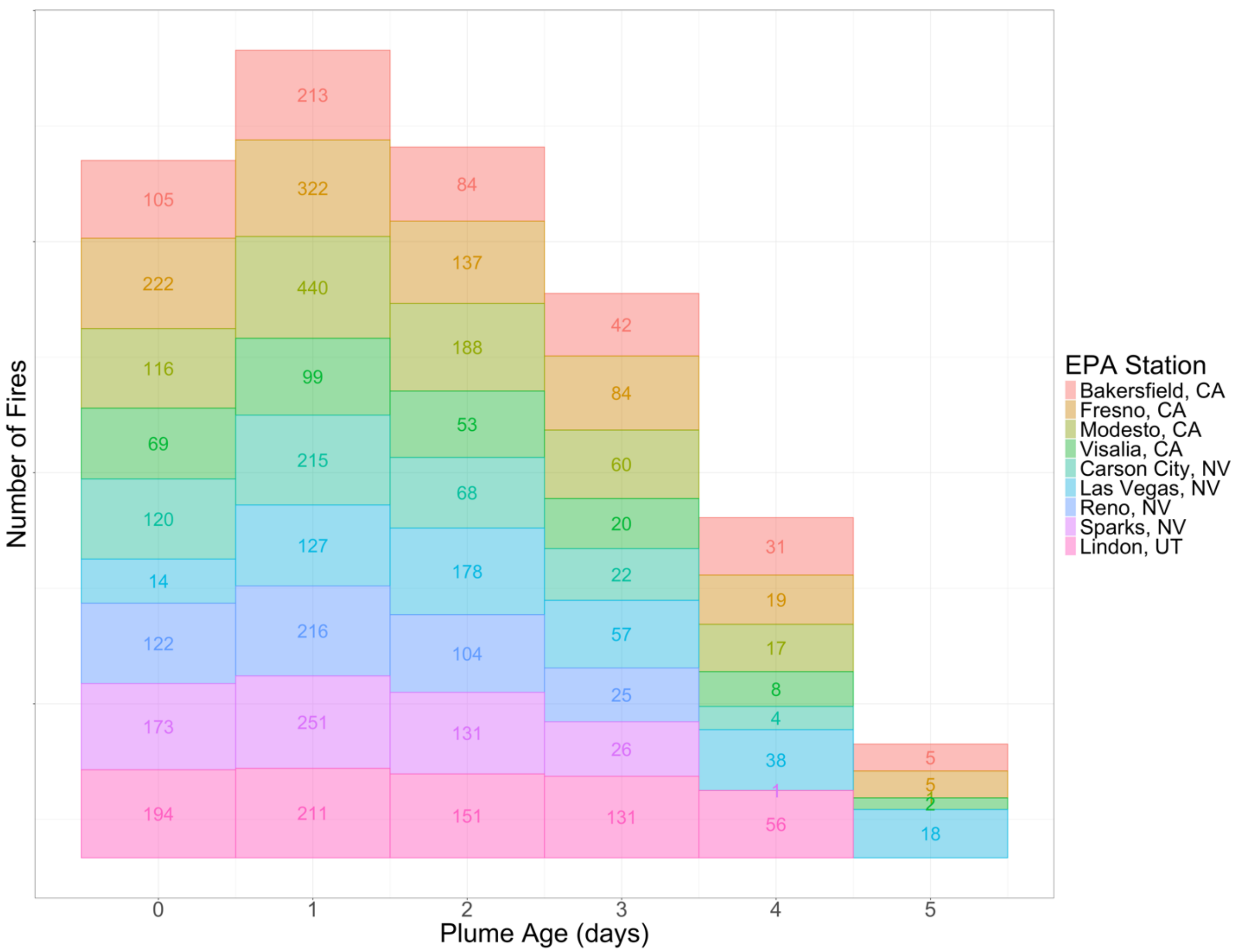

Figure 9. Age of the smoke plume impacting each station in days, determined using an average wind speed value across each state.

References

[1] S. Pan, L. Gan, J. Jung, W. Yu, A. Roy, L. Diao, W. Jeon, A.H. Souri, H.O. Gao, Y. Choi, Quantifying the premature mortality and economic loss from wildfire-induced PM2.5 in the contiguous U.S, Sci. Total Environ. 875 (2023) 162614.

[2] Y. Gao, W. Huang, P. Yu, R. Xu, Z. Yang, D. Gasevic, T. Ye, Y. Guo, S. Li, Long-term impacts of non-occupational wildfire exposure on human health: A systematic review, Environ. Pollut. 320 (2023) 121041.

[3] J.C. Liu, G. Pereira, S.A. Uhl, M.A. Bravo, M.L. Bell, A systematic review of the physical health impacts from non-occupational exposure to wildfire smoke, Environ. Res. 136 (2015) 120–132.

[4] C.E. Reid, M. Brauer, F.H. Johnston, M. Jerrett, J.R. Balmes, C.T. Elliott, Critical Review of Health Impacts of Wildfire Smoke Exposure, Environ. Health Perspect. 124 (2016) 1334–1343.

[5] R. Thilakaratne, S. Hoshiko, A. Rosenberg, T. Hayashi, J.R. Buckman, A.G. Rappold, Wildfires and the Changing Landscape of Air Pollution-related Health Burden in California, Am. J. Respir. Crit. Care Med. (2022). https://doi.org/10.1164/rccm.202207-1324OC.

[6] L. Stawovy, B. Balakrishnan, The Threat of Wildfires and Pulmonary Complications: A Narrative Review, Current Pulmonology Reports (2022). https://doi.org/10.1007/s13665-022-00293-7.

[7] E. Grant, J.D. Runkle, Long-term health effects of wildfire exposure: A scoping review, The Journal of Climate Change and Health 6 (2022) 100110.

[8] R. Meadows, Climate Change, Wildfires, and Health in Canada, in: R. Akhtar (Ed.), Climate Change and Human Health Scenarios: International Case Studies, Springer Nature Switzerland, Cham, 2023: pp. 385–397.

[9] S.E. Cleland, L.H. Wyatt, L. Wei, N. Paul, M.L. Serre, J.J. West, S.B. Henderson, A.G. Rappold, Short-Term Exposure to Wildfire Smoke and PM2.5 and Cognitive Performance in a

Brain-Training Game: A Longitudinal Study of U.S. Adults, Environ. Health Perspect. 130 (06/2022) 067005.

[10] S. Magzamen, R.W. Gan, J. Liu, K. O’Dell, B. Ford, K. Berg, K. Bol, A. Wilson, E.V. Fischer, J.R. Pierce, Differential Cardiopulmonary Health Impacts of Local and Long-Range Transport of Wildfire Smoke, Geohealth 5 (2021) e2020GH000330.

[11] S.M. Loría-Salazar, A. Panorska, W.P. Arnott, J.C. Barnard, J.M. Boehmler, H.A. Holmes, Toward understanding atmospheric physics impacting the relationship between columnar aerosol optical depth and near-surface PM2.5 mass concentrations in Nevada and California, U.S.A., during 2013, Atmos. Environ. 171 (2017) 289–300.

[12] B. Shrestha, J.A. Brotzge, J. Wang, Observations and impacts of long-range transported wildfire smoke on air quality across New York state during July 2021, Geophys. Res. Lett. 49 (2022). https://doi.org/10.1029/2022gl100216.

[13] H.M. Rogers, J.C. Ditto, D.R. Gentner, Evidence for impacts on surface-level air quality in the northeastern US from long-distance transport of smoke from North American fires during the Long Island Sound Tropospheric Ozone Study (LISTOS) 2018, Atmos. Chem. Phys. 20 (2020) 671–682.

[14] W.E. Heilman, Y. Liu, S. Urbanski, V. Kovalev, R. Mickler, Wildland fire emissions, carbon, and climate: Plume rise, atmospheric transport, and chemistry processes, For. Ecol. Manage. 317 (2014) 70–79.

[15] J.C. Liu, L.J. Mickley, M.P. Sulprizio, X. Yue, R.D. Peng, F. Dominici, M.L. Bell, Future respiratory hospital admissions from wildfire smoke under climate change in the Western US, Environ. Res. Lett. 11 (2016) 124018.

[16] J.D. Stowell, C.-E. Yang, J.S. Fu, N.C. Scovronick, M.J. Strickland, Y. Liu, Asthma exacerbation due to climate change-induced wildfire smoke in the Western US, Environ. Res. Lett. 17 (2021) 014023.

[17] F. Reisen, S.M. Duran, M. Flannigan, C. Elliott, K. Rideout, Wildfire smoke and public health risk, Int. J. Wildland Fire 24 (2015) 1029.

[18] B. Ford, M. Val Martin, S.E. Zelasky, E.V. Fischer, S.C. Anenberg, C.L. Heald, J.R. Pierce, Future Fire Impacts on Smoke Concentrations, Visibility, and Health in the Contiguous United States, Geohealth 2 (2018) 229–247.

[19] R.P. Fadadu, B. Grimes, N.P. Jewell, J. Vargo, A.T. Young, K. Abuabara, J.R. Balmes, M.L. Wei, Association of Wildfire Air Pollution and Health Care Use for Atopic Dermatitis and Itch, JAMA Dermatol. 157 (2021) 658–666.

[20] N. Gianniou, C. Giannakopoulou, E. Dima, M. Kardara, P. Katsaounou, A. Tsakatikas, C. Roussos, N. Koulouris, N. Rovina, Acute effects of smoke exposure on airway and systemic inflammation in forest firefighters, J. Asthma Allergy 11 (2018) 81–88.

[21] T. Ye, R. Xu, X. Yue, G. Chen, P. Yu, M.S.Z.S. Coêlho, P.H.N. Saldiva, M.J. Abramson, Y. Guo, S. Li, Short-term exposure to wildfire-related PM2.5 increases mortality risks and burdens in Brazil, Nat. Commun. 13 (2022) 7651.

[22] S. Heft-Neal, C.F. Gould, M. Childs, M.V. Kiang, K. Nadeau, M. Duggan, E. Bendavid, M. Burke, Behavior Mediates the Health Effects of Extreme Wildfire Smoke Events, (2023). https://doi.org/10.3386/w30969.

[23] R.J. Laumbach, Clearing the Air on Personal Interventions to Reduce Exposure to Wildfire Smoke, Ann. Am. Thorac. Soc. 16 (2019) 815–818.

[24] M.B. Hadley, S.B. Henderson, M. Brauer, R. Vedanthan, Protecting Cardiovascular Health From Wildfire Smoke, Circulation 146 (2022) 788–801.

[25] A. Ontawong, S. Saokaew, B. Jamroendararasame, A. Duangjai, Impact of long-term exposure wildfire smog on respiratory health outcomes, Expert Rev. Respir. Med. 14 (2020) 527–531.

[26] R.D. Brook, D.E. Newby, S. Rajagopalan, Air Pollution and Cardiometabolic Disease: An Update and Call for Clinical Trials, Am. J. Hypertens. 31 (2017) 1–10.

[27] C. Black, Y. Tesfaigzi, J.A. Bassein, L.A. Miller, Wildfire smoke exposure and human health: Significant gaps in research for a growing public health issue, Environ. Toxicol. Pharmacol. 55 (2017) 186–195.

[28] L. Giglio, D.P. Roy, On the outstanding need for a long-term, multi-decadal, validated and quality assessed record of global burned area: Caution in the use of Advanced Very High Resolution Radiometer data, Egypt. J. Remote Sens. Space Sci. 2 (2020) 100007.

[29] T.J. Hawbaker, M.K. Vanderhoof, Y.-J. Beal, J.D. Takacs, G.L. Schmidt, J.T. Falgout, B. Williams, N.M. Fairaux, M.K. Caldwell, J.J. Picotte, S.M. Howard, S. Stitt, J.L. Dwyer, Mapping burned areas using dense time-series of Landsat data, Remote Sens. Environ. 198 (2017) 504–522.

[30] T.W. Juliano, N. Lareau, M. Frediani, K. Shamsaei, M. Eghdami, K.A. Kosiba, J. Wurman, A. DeCastro, B. Kosović, H. Ebrahimian, Toward a Better Understanding of Wildfire Behavior in the Wildland-Urban Interface: A Case Study of the 2021 Marshall Fire, Authorea Preprints (2022).

[31] I.N. Sokolik, A.J. Soja, P.J. DeMott, D. Winker, Progress and challenges in quantifying wildfire smoke emissions, their properties, transport, and atmospheric impacts, J. Geophys. Res. 124 (2019) 13005–13025.

[32] W.T. Sommers, R.A. Loehman, C.C. Hardy, Wildland fire emissions, carbon, and climate: Science overview and knowledge needs, For. Ecol. Manage. 317 (2014) 1–8.

[33] T.S. Carter, C.L. Heald, J.L. Jimenez, P. Campuzano-Jost, Y. Kondo, N. Moteki, J.P. Schwarz, C. Wiedinmyer, A.S. Darmenov, A.M. da Silva, J.W. Kaiser, How emissions uncertainty influences the distribution and radiative impacts of smoke from fires in North America, Atmos. Chem. Phys. 20 (2020) 2073–2097.

[34] B. Roy, G.A. Pouliot, A. Gilliland, T. Pierce, S. Howard, P.V. Bhave, W. Benjey, Refining fire emissions for air quality modeling with remotely sensed fire counts: A wildfire case study, Atmos. Environ. 41 (2007) 655–665.

[35] F. Li, X. Zhang, S. Kondragunta, X. Lu, I. Csiszar, C.C. Schmidt, Hourly biomass burning emissions product from blended geostationary and polar-orbiting satellites for air quality forecasting applications, Remote Sens. Environ. 281 (2022) 113237.
[36] N.L. Murray, H.A. Holmes, Y. Liu, H.H. Chang, A Bayesian ensemble approach to combine PM2.5 estimates from statistical models using satellite imagery and numerical model simulation, Environ. Res. 178 (2019) 108601.
[37] J.C. Liu, L.J. Mickley, M.P. Sulprizio, F. Dominici, X. Yue, K. Ebisu, G.B. Anderson, R.F.A. Khan, M.A. Bravo, M.L. Bell, Particulate air pollution from wildfires in the Western US under climate change, Clim. Change 138 (2016) 655–666.
[38] T. Strand, N. Larkin, M. Rorig, C. Krull, M. Moore, PM2.5 measurements in wildfire smoke plumes from fire seasons 2005–2008 in the Northwestern United States, J. Aerosol Sci. 42 (2011) 143–155.
[39] P. Morgan, R.E. Keane, G.K. Dillon, T.B. Jain, A.T. Hudak, E.C. Karau, P.G. Sikkink, Z.A. Holden, E.K. Strand, Challenges of assessing fire and burn severity using field measures, remote sensing and modelling, Int. J. Wildland Fire 23 (2014) 1045.
[40] J.D. Stowell, G. Geng, E. Saikawa, H.H. Chang, J. Fu, C.-E. Yang, Q. Zhu, Y. Liu, M.J. Strickland, Associations of wildfire smoke PM2.5 exposure with cardiorespiratory events in Colorado 2011–2014, Environ. Int. 133 (2019) 105151.
[41] C.E. Stockwell, M.M. Bela, M.M. Coggon, G.I. Gkatzelis, E. Wiggins, E.M. Gargulinski, T. Shingler, M. Fenn, D. Griffin, C.D. Holmes, X. Ye, P.E. Saide, I. Bourgeois, J. Peischl, C.C. Womack, R.A. Washenfelder, P.R. Veres, J.A. Neuman, J.B. Gilman, A. Lamplugh, R.H. Schwantes, S.A. McKeen, A. Wisthaler, F. Piel, H. Guo, P. Campuzano-Jost, J.L. Jimenez, A. Fried, T.F. Hanisco, L.G. Huey, A. Perring, J.M. Katich, G.S. Diskin, J.B. Nowak, T.P. Bui, H.S. Halliday, J.P. DiGangi, G. Pereira, E.P. James, R. Ahmadov, C.A. McLinden, A.J. Soja, R.H. Moore, J.W. Hair, C. Warneke, Airborne emission rate measurements validate remote sensing

observations and emission inventories of western U.s. wildfires, Environ. Sci. Technol. 56 (2022) 7564–7577.

[42] H. Hao, H.H. Chang, H.A. Holmes, J.A. Mulholland, M. Klein, L.A. Darrow, M.J. Strickland, Air Pollution and Preterm Birth in the U.S. State of Georgia (2002-2006): Associations with Concentrations of 11 Ambient Air Pollutants Estimated by Combining Community Multiscale Air Quality Model (CMAQ) Simulations with Stationary Monitor Measurements, Environ. Health Perspect. 124 (2016) 875–880.

[43] W.W. Delp, B.C. Singer, Wildfire Smoke Adjustment Factors for Low-Cost and Professional PM2.5 Monitors with Optical Sensors, Sensors 20 (2020). https://doi.org/10.3390/s20133683.

[44] M.S. Landis, R.W. Long, J. Krug, M. Colón, R. Vanderpool, A. Habel, S.P. Urbanski, The U.S. EPA wildland fire sensor challenge: Performance and evaluation of solver submitted multi-pollutant sensor systems, Atmos. Environ. 247 (2021) 118165.

[45] D.J. Miller, K. Sun, M.A. Zondlo, D. Kanter, Assessing boreal forest fire smoke aerosol impacts on US air quality: A case study using multiple data sets, Journal Of (2011). https://doi.org/10.1029/2011JD016170.

[46] X. Ye, P. Arab, R. Ahmadov, E. James, G.A. Grell, B. Pierce, A. Kumar, P. Makar, J. Chen, D. Davignon, G.R. Carmichael, G. Ferrada, J. McQueen, J. Huang, R. Kumar, L. Emmons, F.L. Herron-Thorpe, M. Parrington, R. Engelen, V.-H. Peuch, A. da Silva, A. Soja, E. Gargulinski, E. Wiggins, J.W. Hair, M. Fenn, T. Shingler, S. Kondragunta, A. Lyapustin, Y. Wang, B. Holben, D.M. Giles, P.E. Saide, Evaluation and intercomparison of wildfire smoke forecasts from multiple modeling systems for the 2019 Williams Flats fire, Atmos. Chem. Phys. 21 (2021) 14427–14469.

[47] R. Aguilera, N. Luo, R. Basu, J. Wu, R. Clemesha, A. Gershunov, T. Benmarhnia, A novel ensemble-based statistical approach to estimate daily wildfire-specific PM2.5 in California (2006–2020), Environ. Int. 171 (2023) 107719.

[48] A.K. Kochanski, D.V. Mallia, M.G. Fearon, J. Mandel, A.H. Souri, T. Brown, Modeling wildfire smoke feedback mechanisms using a coupled fire-atmosphere model with a radiatively active aerosol scheme, J. Geophys. Res. 124 (2019) 9099–9116.
[49] T.Y. Wilmot, D.V. Mallia, A.G. Hallar, J.C. Lin, Wildfire activity is driving summertime air quality degradation across the western US: a model-based attribution to smoke source regions, Environ. Res. Lett. 17 (2022) 114014.
[50] A.K. Smith, S. Dragicevic, AN AGENT-BASED MODEL TO REPRESENT SPACE-TIME PROPAGATION OF FOREST-FIRE SMOKE, ISPRS Ann. Photogramm. Remote Sens. Spatial Inf. Sci. IV–4 (2018) 207–212.
[51] Y. Liu, A. Kochanski, K.R. Baker, W. Mell, R. Linn, R. Paugam, J. Mandel, A. Fournier, M.A. Jenkins, S. Goodrick, G. Achtemeier, F. Zhao, R. Ottmar, N.H.F. French, N. Larkin, T. Brown, A. Hudak, M. Dickinson, B. Potter, C. Clements, S. Urbanski, S. Prichard, A. Watts, D. McNamara, Fire behaviour and smoke modelling: model improvement and measurement needs for next-generation smoke research and forecasting systems, Int. J. Wildland Fire 28 (2019) 570.
[52] Schweizer, D. W., R. Cisneros, Forest fire policy: change conventional thinking of smoke management to prioritize long-term air quality and public health, Air Qual. Atmos. Health 10 (2017) 33–36.
[53] M.L. Smith, G. Chi, Spatial proximity to wildfires as a proxy for measuring PM2.5: A novel method for estimating exposures in rural settings, The Journal of Climate Change and Health 11 (2023) 100219.
[54] S. Hoshiko, J.R. Buckman, C.G. Jones, K.R. Yeomans, A. Mello, R. Thilakaratne, E. Sergienko, K. Allen, L. Bello, A.G. Rappold, Responses to Wildfire and Prescribed Fire Smoke: A Survey of a Medically Vulnerable Adult Population in the Wildland-Urban Interface, Mariposa County, California, Int. J. Environ. Res. Public Health 20 (2023). https://doi.org/10.3390/ijerph20021210.

[55] M. Kelp, M. Carroll, T. Liu, R. Yantosca, H. Hockenberry, L. Mickley, Prescribed burns as a tool to mitigate future wildfire smoke exposure: Lessons for states and rural environmental justice communities, EarthArXiv (2022). https://doi.org/10.31223/x5w36s.
[56] A.M. Pierce, S.M. Loría-Salazar, H.A. Holmes, M.S. Gustin, Investigating horizontal and vertical pollution gradients in the atmosphere associated with an urban location in complex terrain, Reno, Nevada, USA, Atmos. Environ. 196 (2019) 103–117.
[57] F.L. Herron-Thorpe, G.H. Mount, L.K. Emmons, B.K. Lamb, D.A. Jaffe, N.L. Wigder, S.H. Chung, R. Zhang, M.D. Woelfle, J.K. Vaughan, Air quality simulations of wildfires in the Pacific Northwest evaluated with surface and satellite observations during the summers of 2007 and 2008, Atmos. Chem. Phys. 14 (2014) 12533–12551.
[58] A. Sharma, A.C.F. Valdes, Y. Lee, Impact of Wildfires on Meteorology and Air Quality (PM2.5 and O3) over Western United States during September 2017, Atmosphere 13 (2022) 262.
[59] S.P. Urbanski, W.M. Hao, B. Nordgren, The wildland fire emission inventory: western United States emission estimates and an evaluation of uncertainty, Atmos. Chem. Phys. 11 (2011) 12973–13000.
[60] J.D. Redman, H.A. Holmes, S. Balachandran, M.L. Maier, X. Zhai, C. Ivey, K. Digby, J.A. Mulholland, A.G. Russell, Development and evaluation of a daily temporal interpolation model for fine particulate matter species concentrations and source apportionment, Atmos. Environ. 140 (2016) 529–538.
[61] A. van Donkelaar, R.V. Martin, M. Brauer, N.C. Hsu, R.A. Kahn, R.C. Levy, A. Lyapustin, A.M. Sayer, D.M. Winker, Global Estimates of Fine Particulate Matter using a Combined Geophysical-Statistical Method with Information from Satellites, Models, and Monitors, Environ. Sci. Technol. 50 (2016) 3762–3772.

[62] A. van Donkelaar, R.V. Martin, R.J.D. Spurr, R.T. Burnett, High-Resolution Satellite-Derived PM2.5 from Optimal Estimation and Geographically Weighted Regression over North America, Environ. Sci. Technol. 49 (2015) 10482–10491.
[63] H.H. Chang, X. Hu, Y. Liu, Calibrating MODIS aerosol optical depth for predicting daily PM2.5 concentrations via statistical downscaling, J. Expo. Sci. Environ. Epidemiol. 24 (2014) 398–404.
[64] H.A. Holmes, E.R. Pardyjak, Investigation of time-resolved atmospheric conditions and indoor/outdoor particulate matter concentrations in homes with gas and biomass cook stoves in Nogales, Sonora, Mexico, J. Air Waste Manag. Assoc. 64 (2014) 759–773.
[65] C.E. Ivey, H.A. Holmes, Y.T. Hu, Development of PM2.5 source impact spatial fields using a hybrid source apportionment air quality model, Geoscientific Model (2015). https://gmd.copernicus.org/articles/8/2153/2015/.
[66] C.B. Clements, A.J. Oliphant, The California State University Mobile Atmospheric Profiling System: A Facility for Research and Education in Boundary Layer Meteorology, Bull. Am. Meteorol. Soc. 95 (2014) 1713–1724.
[67] M.J. Brewer, C.B. Clements, The 2018 Camp Fire: Meteorological Analysis Using In Situ Observations and Numerical Simulations, Atmosphere 11 (2019) 47.
[68] D.A. Peterson, M.D. Fromm, J.E. Solbrig, E.J. Hyer, M.L. Surratt, J.R. Campbell, Detection and Inventory of Intense Pyroconvection in Western North America using GOES-15 Daytime Infrared Data, J. Appl. Meteorol. Climatol. 56 (2017) 471–493.
[69] D.A. Peterson, E.J. Hyer, J.R. Campbell, M.D. Fromm, J.W. Hair, C.F. Butler, M.A. Fenn, The 2013 Rim Fire: Implications for Predicting Extreme Fire Spread, Pyroconvection, and Smoke Emissions, Bull. Am. Meteorol. Soc. 96 (2015) 229–247.
[70] S.M. Loría-Salazar, A.M. Sayer, J. Barnes, J. Huang, C. Flynn, N. Lareau, J. Lee, A. Lyapustin, J. Redemann, E.J. Welton, J.L. Wilkins, H.A. Holmes, Evaluation of novel NASA moderate resolution imaging spectroradiometer and visible infrared imaging radiometer suite

aerosol products and assessment of smoke height boundary layer ratio during extreme smoke events in the western USA, J. Geophys. Res. 126 (2021). https://doi.org/10.1029/2020jd034180.

[71] S.M. Loría-Salazar, H.A. Holmes, W. Patrick Arnott, J.C. Barnard, H. Moosmüller, Evaluation of MODIS columnar aerosol retrievals using AERONET in semi-arid Nevada and California, U.S.A., during the summer of 2012, Atmos. Environ. 144 (2016) 345–360.

[72] A. Lyapustin, Y. Wang, S. Korkin, D. Huang, MODIS Collection 6 MAIAC algorithm, Atmos. Meas. Tech. 11 (2018) 5741–5765.

[73] M. Brauer, G. Freedman, J. Frostad, A. van Donkelaar, R.V. Martin, F. Dentener, R. van Dingenen, K. Estep, H. Amini, J.S. Apte, K. Balakrishnan, L. Barregard, D. Broday, V. Feigin, S. Ghosh, P.K. Hopke, L.D. Knibbs, Y. Kokubo, Y. Liu, S. Ma, L. Morawska, J.L.T. Sangrador, G. Shaddick, H.R. Anderson, T. Vos, M.H. Forouzanfar, R.T. Burnett, A. Cohen, Ambient Air Pollution Exposure Estimation for the Global Burden of Disease 2013, Environ. Sci. Technol. 50 (2016) 79–88.

[74] A. van Donkelaar, M.S. Hammer, L. Bindle, M. Brauer, J.R. Brook, M.J. Garay, N.C. Hsu, O.V. Kalashnikova, R.A. Kahn, C. Lee, R.C. Levy, A. Lyapustin, A.M. Sayer, R.V. Martin, Monthly Global Estimates of Fine Particulate Matter and Their Uncertainty, Environ. Sci. Technol. 55 (2021) 15287–15300.

[75] C.J. Vernon, R. Bolt, T. Canty, R.A. Kahn, The impact of MISR-derived injection height initialization on wildfire and volcanic plume dispersion in the HYSPLIT model, Atmos. Meas. Tech. 11 (2018) 6289–6307.

[76] R. Paugam, M. Wooster, S. Freitas, M. Val Martin, A review of approaches to estimate wildfire plume injection height within large-scale atmospheric chemical transport models, Atmos. Chem. Phys. 16 (2016) 907–925.

[77] Y. Li, D. Tong, S. Ma, S.R. Freitas, R. Ahmadov, M. Sofiev, X. Zhang, S. Kondragunta, R. Kahn, Y. Tang, B. Baker, P. Campbell, R. Saylor, G. Grell, F. Li, Impacts of estimated plume

rise on $PM_{2.5}$ exceedance prediction during extreme wildfire events: a comparison of three schemes (Briggs, Freitas, and Sofiev), Atmos. Chem. Phys. 23 (2023) 3083–3101.

[78] X. Zhang, S. Kondragunta, J. Ram, C. Schmidt, H.-C. Huang, Near-real-time global biomass burning emissions product from geostationary satellite constellation, J. Geophys. Res. 117 (2012). https://doi.org/10.1029/2012jd017459.

[79] J.L. Wilkins, B. de Foy, A.M. Thompson, D.A. Peterson, E.J. Hyer, C. Graves, J. Fishman, G.A. Morris, Evaluation of stratospheric intrusions and biomass burning plumes on the vertical distribution of tropospheric ozone over the Midwestern United States, J. Geophys. Res. 125 (2020). https://doi.org/10.1029/2020jd032454.

[80] A.F. Stein, R.R. Draxler, G.D. Rolph, B.J.B. Stunder, M.D. Cohen, F. Ngan, NOAA's HYSPLIT atmospheric transport and dispersion modeling system, Bull. Am. Meteorol. Soc. 96 (2015) 2059–2077.

[81] S.R. Schneider, K. Lee, G. Santos, J.P.D. Abbatt, Air Quality Data Approach for Defining Wildfire Influence: Impacts on PM2.5, NO2, CO, and O3 in Western Canadian Cities, Environ. Sci. Technol. 55 (2021) 13709–13717.

[82] E. de Souza Fernandes Duarte, M.J. Costa, V.C. Salgueiro, P.S. Lucio, M. Potes, D. Bortoli, R. Salgado, Fire-Pollutant-Atmosphere Interaction and Its Impact on Mortality in Portugal During Wildfire Seasons, Authorea Preprints (2022). https://doi.org/10.1002/essoar.10512142.1.

[83] R. Draxler, B. Stunder, G. Rolph, A. Stein, A. Taylor, S. Zinn, C. Loughner, A. Crawford, HYSPLIT User's Guide Version 5, (2020). https://www.ready.noaa.gov/hysplitusersguide/S417.htm (accessed February 23, 2021).

[84] M. Sicard, M.J. Granados-Muñoz, L. Alados-Arboledas, R. Barragán, A.E. Bedoya-Velásquez, J.A. Benavent-Oltra, D. Bortoli, A. Comerón, C. Córdoba-Jabonero, M.J. Costa, A. del Águila, A.J. Fernández, J.L. Guerrero-Rascado, O. Jorba, F. Molero, C. Muñoz-Porcar, P. Ortiz-Amezcua, N. Papagiannopoulos, M. Potes, M. Pujadas, F. Rocadenbosch, A. Rodríguez-

Gómez, R. Román, R. Salgado, V. Salgueiro, Y. Sola, M. Yela, Ground/space, passive/active remote sensing observations coupled with particle dispersion modelling to understand the inter-continental transport of wildfire smoke plumes, Remote Sens. Environ. 232 (2019) 111294.
[85] G.D. Rolph, R.R. Draxler, A.F. Stein, A. Taylor, M.G. Ruminski, S. Kondragunta, J. Zeng, H.-C. Huang, G. Manikin, J.T. McQueen, P.M. Davidson, Description and Verification of the NOAA Smoke Forecasting System: The 2007 Fire Season, Weather Forecast. 24 (2009) 361–378.
[86] S. Faulstich, M. Strickland, H. Holmes, Enhancing fire emissions inventories for acute health effects studies: Integrating high spatial and temporal resolution data, Int. J. Wildland Fire (2025) Accepted.
[87] N.H.F. French, D. McKenzie, T. Erickson, B. Koziol, M. Billmire, K.A. Endsley, N.K. Yager Scheinerman, L. Jenkins, M.E. Miller, R. Ottmar, S. Prichard, Modeling Regional-Scale Wildland Fire Emissions with the Wildland Fire Emissions Information System*, Earth Interact. 18 (2014) 1–26.
[88] National Centers for Environmental Prediction/National Weather Service/NOAA/U.S. Department of Commerce, NCEP North American Mesoscale (NAM) 12 km Analysis, (2015). https://doi.org/10.5065/G4RC-1N91.
[89] G.A. Briggs, Plume rise: A critical survey, Office of Scientific and Technical Information (OSTI), 1969. https://doi.org/10.2172/4743102.
[90] Y. Wu, C.-M. Gan, B. Gross, F. Moshary, S. Ahmed, Aerosol plume observations by the ground-based lidar, sunphotometer, and satellite: cases analysis, in: U.N. Singh, G. Pappalardo (Eds.), Lidar Technologies, Techniques, and Measurements for Atmospheric Remote Sensing V, SPIE, 2009. https://doi.org/10.1117/12.830639.
[91] S.L. Scott, H.R. Varian, Predicting the present with Bayesian structural time series, International Journal of Mathematical Modelling and Numerical Optimisation 5 (2014) 4–23.

[92] J. Horel, M. Splitt, L. Dunn, J. Pechmann, B. White, C. Ciliberti, S. Lazarus, J. Slemmer, D. Zaff, J. Burks, MESOWEST: COOPERATIVE MESONETS IN THE WESTERN UNITED STATES, Bull. Am. Meteorol. Soc. 83 (2002) 211–226.

[93] S. Wang, P.J. Gallimore, C. Liu-Kang, K. Yeung, S.J. Campbell, B. Utinger, T. Liu, H. Peng, M. Kalberer, A.W.H. Chan, J.P.D. Abbatt, Dynamic Wood Smoke Aerosol Toxicity during Oxidative Atmospheric Aging, Environ. Sci. Technol. (2023). https://doi.org/10.1021/acs.est.2c05929.

[94] Y. Liang, C.N. Jen, R.J. Weber, P.K. Misztal, A.H. Goldstein, Chemical composition of $PM_{2.5}$ in October 2017 Northern California wildfire plumes, Atmos. Chem. Phys. 21 (2021) 5719–5737.

[95] K. O'Dell, R.S. Hornbrook, W. Permar, E.J.T. Levin, L.A. Garofalo, E.C. Apel, N.J. Blake, A. Jarnot, M.A. Pothier, D.K. Farmer, L. Hu, T. Campos, B. Ford, J.R. Pierce, E.V. Fischer, Hazardous Air Pollutants in Fresh and Aged Western US Wildfire Smoke and Implications for Long-Term Exposure, Environ. Sci. Technol. 54 (2020) 11838–11847.

[96] J.B. Simmons, C. Paton-Walsh, A.P. Mouat, J. Kaiser, R.S. Humphries, M. Keywood, D.W.T. Griffith, A. Sutresna, T. Naylor, J. Ramirez-Gamboa, Bushfire smoke plume composition and toxicological assessment from the 2019–2020 Australian Black Summer, Air Qual. Atmos. Health (2022). https://doi.org/10.1007/s11869-022-01237-5.

[97] S.L. Altshuler, Q. Zhang, M.T. Kleinman, F. Garcia-Menendez, C.T.T. Moore, M.L. Hough, E.D. Stevenson, J.C. Chow, D.A. Jaffe, J.G. Watson, Wildfire and prescribed burning impacts on air quality in the United States, J. Air Waste Manag. Assoc. 70 (2020) 961–970.

[98] Schweizer, Don, H.K. Preisler, R. Cisneros, Assessing relative differences in smoke exposure from prescribed, managed, and full suppression wildland fire, Air Qual. Atmos. Health 12 (2019) 87–95.

[99] Y.H. Kim, S.H. Warren, Q.T. Krantz, C. King, R. Jaskot, W.T. Preston, B.J. George, M.D. Hays, M.S. Landis, M. Higuchi, D.M. DeMarini, M.I. Gilmour, Mutagenicity and Lung Toxicity of

Smoldering vs. Flaming Emissions from Various Biomass Fuels: Implications for Health Effects from Wildland Fires, Environ. Health Perspect. 126 (2018) 017011.

[100] L.E. Koval, C.K. Carberry, Y.H. Kim, E. McDermott, H. Hartwell, I. Jaspers, M.I. Gilmour, J.E. Rager, Wildfire Variable Toxicity: Identifying Biomass Smoke Exposure Groupings through Transcriptomic Similarity Scoring, Environ. Sci. Technol. 56 (2022) 17131–17142.

[101] M.M. Ahmed, A. Trouvé, J. Forthofer, M. Finney, Simulations of flaming combustion and flaming-to-smoldering transition in wildland fire spread at flame scale, Combust. Flame 262 (2024) 113370.

[102] M.A. Santoso, E.G. Christensen, J. Yang, G. Rein, Review of the Transition From Smouldering to Flaming Combustion in Wildfires, Front. Mech. Eng. Chin. 5 (2019). https://doi.org/10.3389/fmech.2019.00049.

[103] C.L. Riccardi, S.J. Prichard, D.V. Sandberg, R.D. Ottmar, Quantifying physical characteristics of wildland fuels using the Fuel Characteristic Classification SystemThis article is one of a selection of papers published in the Special Forum on the Fuel Characteristic Classification System, Can. J. For. Res. 37 (2007) 2413–2420.

[104] B.R. Parresol, J.I. Blake, A.J. Thompson, Effects of overstory composition and prescribed fire on fuel loading across a heterogeneous managed landscape in the southeastern USA, For. Ecol. Manage. 273 (2012) 29–42.

[105] J.K. McDaniel, H.D. Alexander, C.M. Siegert, M.A. Lashley, Shifting tree species composition of upland oak forests alters leaf litter structure, moisture, and flammability, For. Ecol. Manage. 482 (2021) 118860.

[106] C. Homer, C. Huang, L. Yang, B. Wylie, M. Coan, Development of a 2001 National Land-Cover Database for the United States, Photogrammetric Engineering & Remote Sensing 70 (2004) 829–840.

[107] Y. Liu, E. Austin, J. Xiang, T. Gould, T. Larson, E. Seto, Health impact assessment of the 2020 Washington state wildfire smoke episode: Excess health burden attributable to

increased PM2.5 exposures and potential exposure reductions, GeoHealth 5 (2021) e2020GH000359.

[108] Western Regional Climate Center Average Wind Speeds Comparative Table, (2006). https://wrcc.dri.edu/Climate/comp_table_show.php?stype=wind_speed_avg (accessed July 15, 2024).

[109] World Health Organization, WHO global air quality guidelines: particulate matter (PM2.5 and PM10), ozone, nitrogen dioxide, sulfur dioxide and carbon monoxide, (2021). https://www.who.int/publications/i/item/9789240034228 (accessed December 15, 2024).

[110] HYSPLIT Model Updates, Air Resources Laboratory (n.d.). https://www.arl.noaa.gov/hysplit/hysplit-model-updates/ (accessed April 13, 2025).

[111] S.K. Akagi, R.J. Yokelson, C. Wiedinmyer, M.J. Alvarado, J.S. Reid, T. Karl, J.D. Crounse, P.O. Wennberg, Emission factors for open and domestic biomass burning for use in atmospheric models, Atmos. Chem. Phys. 11 (2011) 4039–4072.

[112] J.S. Reid, R. Koppmann, T.F. Eck, D.P. Eleuterio, A review of biomass burning emissions part II: intensive physical properties of biomass burning particles, Atmos. Chem. Phys. (2005) 27.

[113] K.A. Pratt, S.M. Murphy, R. Subramanian, P.J. DeMott, G.L. Kok, T. Campos, D.C. Rogers, A.J. Prenni, A.J. Heymsfield, J.H. Seinfeld, K.A. Prather, Flight-based chemical characterization of biomass burning aerosols within two prescribed burn smoke plumes, Atmos. Chem. Phys. 11 (2011) 12549–12565.

[114] C.F. Cahill, T.A. Cahill, K.D. Perry, The size- and time-resolved composition of aerosols from a sub-Arctic boreal forest prescribed burn, Atmos. Environ. (1994) 42 (2008) 7553–7559.

[115] D. Cleaves, T. Haines, J. Martinez, Prescribed burning costs: Trends and influences in the National Forest system, USDA Forest Service, 2007. https://www.fs.usda.gov/psw/publications/documents/psw_gtr173/psw_gtr173_06_cleaves.pdf.

[116] United States Census Bureau > Communications Directorate - Center for New Media, QuickFacts: Tulare County, California, (n.d.). https://www.census.gov/quickfacts/fact/table/tularecountycalifornia/PST045223 (accessed October 31, 2024).

[117] C. Reid, E. Considine, G. Watson, D. Telesca, G. Pfister, M. Jerrett, Effect modification of the association between fine particulate air pollution during a wildfire event and respiratory health by area-level measures of socio-economic status, race/ethnicity, and smoking prevalence, Environ. Res.: Health (2023). https://doi.org/10.1088/2752-5309/acc4e1.

[118] C. Bhattarai, V. Samburova, D. Sengupta, M. Iaukea-Lum, A.C. Watts, H. Moosmüller, A.Y. Khlystov, Physical and chemical characterization of aerosol in fresh and aged emissions from open combustion of biomass fuels, Aerosol Sci. Technol. 52 (2018) 1266–1282.

[119] P.D. Koman, M. Billmire, K.R. Baker, R. de Majo, F.J. Anderson, S. Hoshiko, B.J. Thelen, N.H.F. French, Mapping Modeled Exposure of Wildland Fire Smoke for Human Health Studies in California, Atmosphere 10 (2019). https://doi.org/10.3390/atmos10060308.

[120] F.H. Johnston, S.B. Henderson, Y. Chen, J.T. Randerson, M. Marlier, R.S. Defries, P. Kinney, D.M.J.S. Bowman, M. Brauer, Estimated Global Mortality Attributable to Smoke from Landscape Fires, Environ. Health Perspect. 120 (2012) 695–701.

[121] A. Heaney, J.D. Stowell, J.C. Liu, R. Basu, M. Marlier, P. Kinney, Impacts of Fine Particulate Matter From Wildfire Smoke on Respiratory and Cardiovascular Health in California, Geohealth 6 (2022) e2021GH000578.

[122] V. Do, C. Chen, T. Benmarhnia, J.A. Casey, Spatial heterogeneity of the respiratory health impacts of wildfire smoke PM2.5 in California, Authorea Preprints (2023). https://doi.org/10.22541/essoar.170365390.02720545/v1.

[123] S.B. Henderson, M. Brauer, Y.C. MacNab, S.M. Kennedy, Three Measures of Forest Fire Smoke Exposure and Their Associations with Respiratory and Cardiovascular Health Outcomes in a Population-Based Cohort, Environ. Health Perspect. 119 (2011) 1266–1271.

[124] M.L. Childs, J. Li, J. Wen, S. Heft-Neal, A. Driscoll, S. Wang, C.F. Gould, M. Qiu, J. Burney, M. Burke, Daily Local-Level Estimates of Ambient Wildfire Smoke PM2.5 for the Contiguous US, Environ. Sci. Technol. 56 (2022) 13607–13621.

[125] Y. Liu, E. Austin, J. Xiang, T. Gould, T. Larson, E. Seto, Health Impact Assessment of PM2.5 attributable mortality from the September 2020 Washington State Wildfire Smoke Episode, MedRxiv (2020). https://doi.org/10.1101/2020.09.19.20197921.

[126] J. Castagna, A. Senatore, M. Bencardino, G. Mendicino, Concurrent influence of different natural sources on the particulate matter in the central Mediterranean region during a wildfire season, Atmosphere (Basel) 12 (2021) 144.

[127] C.L. Schollaert, J. Jung, J. Wilkins, E. Alvarado, J. Baumgartner, J. Brun, T. Busch Isaksen, J.M. Lydersen, M.E. Marlier, J.D. Marshall, Y.J. Masuda, C. Maxwell, C.W. Tessum, K.N. Wilson, N.H. Wolff, J.T. Spector, Quantifying the smoke-related public health trade-offs of forest management, Nature Sustainability (2023) 1–10.